Sister Kinetochore Recapture in Fission Yeast Occurs by Two Distinct Mechanisms, Both Requiring Dam1 and Klp2

Yannick Gachet, Céline Reyes, Thibault Courthéoux, Sherilyn Goldstone, Guillaume Gay, Céline Serrurier, Sylvie Tournier

Molecular Biology of the Cell
Vol. 19, 1646–1662, April 2008

Sister Kinetochore Recapture in Fission Yeast Occurs by Two Distinct Mechanisms, Both Requiring Dam1 and Klp2

Yannick Gachet,* Céline Reyes,* Thibault Courthéoux, Sherilyn Goldstone, Guillaume Gay, Céline Serrurier, and Sylvie Tournier

Laboratoire de Biologie Cellulaire et Moléculaire du Controle de la Prolifération (LBCMCP), Centre National de la Recherche Scientifique, Université de Toulouse, 31062 Toulouse, France

Submitted September 17, 2007; Revised January 17, 2008; Accepted January 30, 2008
Monitoring Editor: David Drubin

In eukaryotic cells, proper formation of the spindle is necessary for successful cell division. We have studied chromosome recapture in the fission yeast *Schizosaccharomyces pombe*. We show by live cell analysis that lost kinetochores interact laterally with intranuclear microtubules (INMs) and that both microtubule depolymerization (end-on pulling) and minus-end–directed movement (microtubule sliding) contribute to chromosome retrieval to the spindle pole body (SPB). We find that the minus-end–directed motor Klp2 colocalizes with the kinetochore during its transport to the SPB and contributes to the effectiveness of retrieval by affecting both end-on pulling and lateral sliding. Furthermore, we provide in vivo evidence that Dam1, a component of the DASH complex, also colocalizes with the kinetochore during its transport and is essential for its retrieval by either of these mechanisms. Finally, we find that the position of the unattached kinetochore correlates with the size and orientation of the INMs, suggesting that chromosome recapture may not be a random process.

INTRODUCTION

In all eukaryotes, faithful sister chromatid segregation is a key event in the maintenance of genetic integrity. For high-fidelity chromosome segregation, kinetochore attachment to the spindle microtubules is essential and requires microtubule function during mitosis (McIntosh *et al.*, 2002; Maiato *et al.*, 2004).

The capture of the kinetochores by microtubules is an early step in mitosis. This process has been visualized in very few cell types, including the asymmetrically dividing budding yeast (Merdes and De Mey, 1990; Rieder and Alexander, 1990; Tanaka *et al.*, 2005, 2007). In these studies it has been established that the kinetochores are initially captured by either the lateral surface or by the plus-end extremity of a single microtubule extending from a spindle pole. The captured kinetochores are then transported poleward to the spindle pole where each sister kinetochore eventually attaches to the plus ends of microtubules extending from the opposite spindle pole. In the following stage, the chromosomes align at the metaphase plate, which is formed equidistant between the centrosomes. Congression to the metaphase plate is generated by forces produced by kinetochore-bound molecular motors such as the mitotic kinesins. It has also been suggested that chromosome congression is driven by minus-end–directed motors, which can pull the kinetochores from one pole to the opposite one (Savoian *et al.*, 2000; Sharp *et al.*, 2000).

Model organisms have proven to be powerful tools to study the mechanisms that control spindle formation. In both budding and fission yeasts, chromosome segregation occurs within the nuclear envelope (closed mitosis). In *Schizosaccharomyces pombe*, as opposed to budding yeast, spindle formation occurs only in mitosis and multiple microtubule attachment sites are present on the mitotic kinetochores, as is the case in higher eukaryotic cells. Furthermore, because *S. pombe* possesses only three chromosomes, it provides a particularly attractive model for the visualization of kinetochore dynamics and chromosome segregation during mitosis (Tournier *et al.*, 2004; Courtheoux *et al.*, 2007).

In budding yeast, the transport of captured kinetochores along microtubules is promoted by Kar3, a kinesin-14 family member, whereas the minus-end–directed motor protein dynein plays no role in this process. However, in the majority of Kar3Δ cells kinetochores are transported efficiently to the spindle pole body (SPB), suggesting that alternative mechanisms probably act redundantly with Kar3. Indeed, it has recently been shown that two mechanisms are involved in poleward kinetochore transport in budding yeast, sliding and end-on pulling (Tanaka *et al.*, 2007).

Recently, Grishchuk and McIntosh (2006) described the mechanisms that control kinetochore retrieval in fission yeast and found that the maximum rate of poleward kinetochore movement was unaffected by the deletion of any or all of the minus-end–directed motors: Klp2 (Kar3 homolog), Pkl1, and dynein. These results strongly suggest that microtubule (MT) depolymerization (end-on pulling) is the only mechanism operating in fission yeast. Unfortunately, in this study the authors were unable to show direct kinetochore–microtubule interactions and therefore how the distant kinetochore moves toward the spindle pole.

The DASH complex, also called the Dam1 complex, is necessary for faithful segregation of chromosomes in mitosis. In budding yeast this complex consists of 10 essential subunits, including Dam1 (Cheeseman *et al.*, 2001, 2002; Janke *et al.*, 2002; Li *et al.*, 2002, 2005). Loss of DASH complex

This article was published online ahead of print in *MBC in Press* (http://www.molbiolcell.org/cgi/doi/10.1091/mbc.E07–09–0910) on February 6, 2008.

* These authors contributed equally to this work.

Address correspondence to: Sylvie Tournier (tournier@cict.fr).

function results in unequal sister chromatid segregation. The homologous complex in fission yeast contains similar subunits and localizes both to the kinetochores and the MT plus ends (Liu *et al.*, 2005; Sanchez-Perez *et al.*, 2005). Although the DASH complex is not essential in fission yeast, its loss also results in abnormal chromosome segregation. It has been previously shown that the DASH complex forms closed rings around MTs (Miranda *et al.*, 2005; Westermann *et al.*, 2006; Wang *et al.*, 2007). It is thought that this ring structure observed in vitro contributes to proper segregation by acting as a processivity factor for the kinetochores, allowing the chromosomes to remain attached to depolymerizing MT plus ends during anaphase. A very recent study has revealed that Dam1 colocalizes with the lost kinetochore on the end of a depolymerizing microtubule and that end-on pulling is compromised in a *dam1* mutant (Tanaka *et al.*, 2007). However, whether Dam1 is sufficient for end-on retrieval has not been established.

In the present study we have addressed the mechanisms of kinetochore recapture in fission yeast. In doing so we show that intranuclear microtubules (INMs) are required to recapture lost kinetochores. We show that kinetochore retrieval is achieved by two mechanisms, either microtubule depolymerization or lateral interaction between the lost kinetochore and the INM, followed by sliding of the kinetochore along the INM toward the SPB. We show that the minus-end–directed motor Klp2 participates in both lateral sliding and microtubule depolymerization, whereas Dam1 is absolutely essential for kinetochore retrieval by either of these mechanisms. Finally, these experiments provide the first in vivo evidence that INMs are preferentially stabilized in the direction of the lost kinetochore, suggesting that unattached chromosomes may generate signals to prevent chromosome loss.

MATERIALS AND METHODS

Cell Culture

Media, growth, maintenance of strains and genetic methods were as described (Moreno *et al.*, 1991). Cells were grown at 25°C in yeast extract. The different strains used in this study are listed in Table 1.

Cell Synchronization and Cold Shock Experiments

Exponentially growing cultures of *cdc25-22* cells at 25°C were arrested in G2 by incubation at 36°C for 4 h and then released into mitosis by rapid cooling to 25°C. Twenty minutes after release, the cells were transferred to 4°C for 30 min, until the mitotic apparatus collapsed. This cold shock was immediately (within 1 min) followed by live microscopy at 25°C.

Cell Fixation

For the statistical analysis of the lost kinetochore-SPB distances and the timing of kinetochore retrieval, cells were fixed in 3.7% formaldehyde for 10 min at room temperature, washed once in phosphate-buffered saline (PBS), and observed after staining with DAPI. A lost kinetochore is defined as a kinetochore that is not located on the spindle in between the two SPBs, but instead at a distance of at least 0.4 μm from the nearest SPB.

Cell Imaging

Live cell analysis was performed in an imaging chamber (CoverWell PCI-2.5, Grace Bio-Labs, Bend, OR) filled with 1 ml of 1% agarose in minimal medium and sealed with a 22 × 22-mm glass coverslip. For the kinetochore retrieval experiments, an aliquot of ice-cold cell suspension was applied to the prewarmed imaging chamber, and the imaging process was begun immediately. Time-lapse images of Z stacks (maximum five stacks of 0.3–0.4-μm steps, to avoid photobleaching) were taken at 15-s intervals or as indicated in the relevant figure legend. Exposure times were 300–500 ms with a HIGHlite light source (Roper Scientific, Evry, France) reduced to 30% to avoid phototoxicity and photobleaching of the MTs. Either the image with the best focal plane or projected images were prepared for each time point. Images were visualized with a Princeton CCD CoolSNAP HQ camera (Roper Scientific) fitted to a Leica DM6000 upright microscope (Leica Microsystems, Rueil-Malmaison, France) with a 100× (1.33 NA) objective and SEMROCK filters, and were recorded using the Metamorph software package (Molecular Devices France, St. Gregoire, France). Intensity adjustments were made using the Metamorph, Image J (http://rsb.info.nih.gov/ij/), and Adobe Photoshop packages (Adobe Systems France, Paris, France). Three-dimensional (3D) reconstructions were performed using the Image J-3D package.

Analysis of Kinetochore and Microtubule Dynamics

The position of the spindle poles and kinetochores were determined using Metamorph and downloaded into Microsoft Excel (Microsoft France, Courtaboeuf, France) or IGOR Pro5.06 (WaveMetrics, Lake Oswego, OR) for analysis. The length of the microtubules, the distance of the kinetochore to the proximal SPB, and the angles with respect to the spindle axis were determined using Metamorph or Image J software. The maximum speed of kinetochore retrieval was determined by plotting the curve of the distance of the kinetochore to the SPB as a function of the time by determining the maximum slope during kinetochore retrieval (using a minimum of three linear time points). The same type of analysis was performed to analyze the INM shrinkage rate. To determine the mode of transport of the kinetochore, cells were scored as either "lateral sliding," defined as when the kinetochore reached the SPB at least 30 s before the end of the INM, or "end-on pulling," when the kinetochore and the end of the INM moved to the SPB simultaneously.

RESULTS

Astral Microtubules and INMs Are Decorated by Different Plus-End Microtubule-tracking Proteins

In fission yeast, different types of nonspindle microtubules, the cytoplasmic microtubules and the INMs, are present during mitosis. Although cytoplasmic microtubules are required to correct spindle orientation, the role of the INMs remains elusive (Gachet *et al.*, 2004; Tolic-Norrelykke *et al.*, 2004; Zimmerman *et al.*, 2004). We first decided to analyze if

Table 1. Strains used in this study

Strain no	Genotype	Reference
ST382	*SV40-gfp-atb2:LEU2 leu1-32*	P. Nurse
ST385	*amo1-rfp:kanR SV40-gfp-atb2:LEU2*	P. Nurse
ST447	*amo1-rfp:kanR mal3-pk-gfp:ura4 leu1-32*	This study
ST509	*ask1-gfp:kanR amo1-rfp:kanR leu1-32 ura4-D18 + pREP-nmt1-ura4-cfp-atb2*	This study
ST665	*cdc25-22 amo1-rfp:kanR ndc80-gfp:kanR cdc11-cfp:kanR SV40-gfp-atb2:LEU2 ura4-D18*	This study
ST697	*dhc1-d1::ura cdc25-22 amo1-rfp:kanR ndc80-gfp:kanR cdc11-cfp:kanR SV40-gfp-atb2:LEU2 ura4-D18*	This study
ST698	*SV40-gfp-atb2:LEU2 ura4-D18*	This study
ST738	*dam1::hyg amo1-rfp:kanR ndc80-gfp:kanR cdc11-cfp:kanR SV40-gfp-atb2:LEU2 ura4-D18*	This study
ST807	*dhc1-d3::LEU2 klp2::ura cdc25-22 ndc80-gfp:kanR cdc11-cfp:kanR SV40-gfp-atb2:LEU2 ura4-D18*	This study
ST809	*cdc25-22 dam1-gfp:kanR ndc80-cfp:kanR*	This study
ST801	*cdc25-22 klp2:pk-gfp:ura ndc80-cfp:kanR cdc11-cfp:kanR*	This study
ST808	*klp2::ura cdc25-22 dam1-gfp:kanR ndc80-cfp:kanR cdc11-cfp:kanR*	This study

these two types of microtubules were "molecularly" different. The distribution of the plus-end microtubule tracking proteins (+TIPs) on these two types of microtubules was an obvious starting point, because the role of the +TIPs in the control of microtubule dynamics, cell polarity, astral microtubule-cortical interactions, and kinetochore–microtubule attachment has been extensively described in various organisms (Wu *et al.*, 2006). Thus, we examined the distributions of the +TIP Mal3, an EB1 family member (Beinhauer *et al.*, 1997; Browning *et al.*, 2003; Busch and Brunner, 2004), and the DASH component Ask1 (Liu *et al.*, 2005), required for correct kinetochore–microtubule attachment, on the INMs and astral microtubules. Using a *mal3-gfp amo1-rfp* strain (+TIP together with a nuclear envelope marker), we found that Mal3 was present on the spindle microtubules and also on both the astral microtubules and the INMs in metaphase cells (Figure 1A; Metaphase). This observation was confirmed by 3D reconstruction of images of a *mal3-gfp amo1-rfp*–expressing cell, which clearly revealed spots of Mal3 (black arrows) that were not aligned with the spindle, although they were located inside the nuclear envelope (Supplementary Figure 1). We noticed that a single dot of Mal3 decorated the preanaphase astral microtubules and INMs, which suggests that at this stage of mitosis few microtubules emanate from the SPB, rather than multiple microtubules. In contrast, after the onset of anaphase the astral microtubules were always decorated by multiple Mal3 dots, suggesting that multiple microtubules are present at this stage (Figure 1A). The same analysis was performed using an *ask1-gfp amo1-rfp atb2-cfp* strain (+TIP, nuclear envelope and tubulin). In contrast to Mal3, we found that during early mitosis

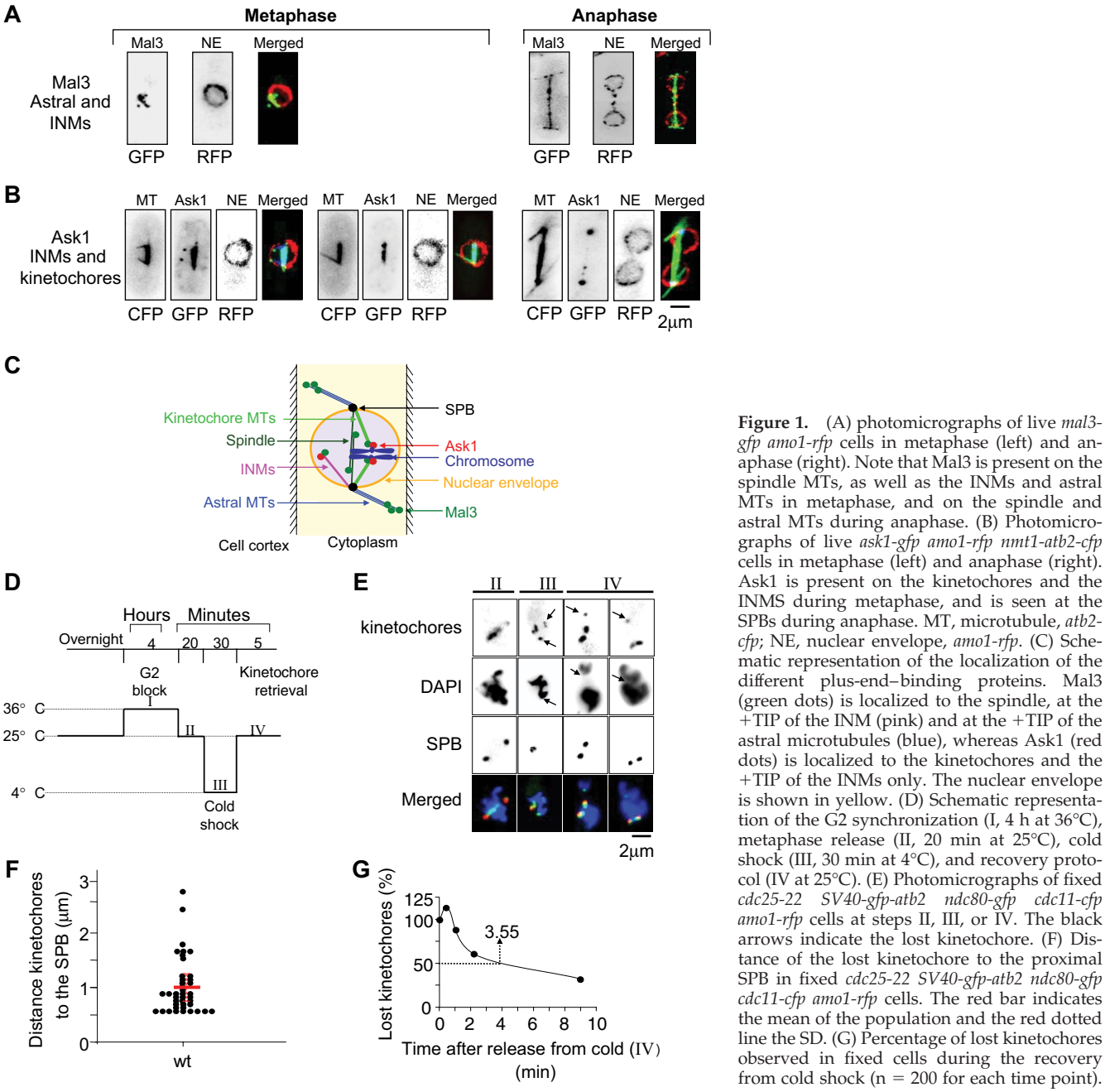

Figure 1. (A) photomicrographs of live *mal3-gfp amo1-rfp* cells in metaphase (left) and anaphase (right). Note that Mal3 is present on the spindle MTs, as well as the INMs and astral MTs in metaphase, and on the spindle and astral MTs during anaphase. (B) Photomicrographs of live *ask1-gfp amo1-rfp nmt1-atb2-cfp* cells in metaphase (left) and anaphase (right). Ask1 is present on the kinetochores and the INMS during metaphase, and is seen at the SPBs during anaphase. MT, microtubule, *atb2-cfp*; NE, nuclear envelope, *amo1-rfp*. (C) Schematic representation of the localization of the different plus-end–binding proteins. Mal3 (green dots) is localized to the spindle, at the +TIP of the INM (pink) and at the +TIP of the astral microtubules (blue), whereas Ask1 (red dots) is localized to the kinetochores and the +TIP of the INMs only. The nuclear envelope is shown in yellow. (D) Schematic representation of the G2 synchronization (I, 4 h at 36°C), metaphase release (II, 20 min at 25°C), cold shock (III, 30 min at 4°C), and recovery protocol (IV at 25°C). (E) Photomicrographs of fixed *cdc25-22 SV40-gfp-atb2 ndc80-gfp cdc11-cfp amo1-rfp* cells at steps II, III, or IV. The black arrows indicate the lost kinetochore. (F) Distance of the lost kinetochore to the proximal SPB in fixed *cdc25-22 SV40-gfp-atb2 ndc80-gfp cdc11-cfp amo1-rfp* cells. The red bar indicates the mean of the population and the red dotted line the SD. (G) Percentage of lost kinetochores observed in fixed cells during the recovery from cold shock (n = 200 for each time point).

Ask1 was exclusively present on the INMs and on spots distributed between the two SPBs, most probably the plus ends of microtubules, which may or may not be attached to a kinetochore. Ask1 was never detected on the astral microtubules (Figure 1B). After the onset of anaphase, although astral microtubules were present, as judged by the Atb2-cfp signal, Ask1 was exclusively located on the SPBs (i.e., the segregated kinetochores) and was never seen on the astral microtubules (n = 200). Identical results were obtained for another DASH component, Dam1, which also exclusively decorated the INMs (data not shown; see also Sanchez-Perez *et al.*, 2005). As summarized in Figure 1C, these observations show that the plus ends of the astral microtubules and the INMs differ at the molecular level.

Visualizing the Retrieval of "Lost" Kinetochores

Because components of the DASH complex localize at the +end of the INMs, we hypothesized that the INMs could be kinetochore microtubules required to prevent chromosome loss in fission yeast cells. To test this hypothesis we analyzed the capture and retrieval of kinetochores (Figure 1D). To do this, we took advantage of a temperature-sensitive fission yeast strain, *cdc25-22,* which arrests in G2 after incubation for 4 h at the restrictive temperature of 36°C, because of its failure to activate Cdc2. Once released from the G2 arrest, by shifting down to the permissive temperature of 25°C, these cells enter mitosis rapidly and with a high degree of synchrony, which considerably facilitates the observation of early mitotic events such as kinetochore capture. We performed a block-and-release experiment using a *cdc25-22 SV40-gfp-atb2 ndc80-gfp cdc11-cfp amo1-rfp* strain, which allowed us to simultaneously visualize the spindle and the INMs (gfp-Atb2), nuclear envelope (Amo1-rfp), kinetochores (Ndc80-gfp), and SPBs (Cdc11-cfp) in a population enriched in metaphase cells. Fission yeast contains only three chromosome pairs (i.e., six chromosomes during mitosis), which can easily be distinguished during metaphase and anaphase A. Importantly, both the microtubules (green lines) and the kinetochores (green dots) were visualized with a green fluorescent protein (GFP)-tagged strain in order to prevent excessive time lapse during filter wheel rotation, which might alter our conclusions on the positions of the kinetochores in respect to the microtubule (side-on or end-on).

The cells were arrested in G2 by incubation at 36°C (Figure 1D, step I) then released into mitosis by rapid cooling to 25°C. After 20 min, 90% of the cell population displayed metaphase spindles (between 1.5 and 2.5 μm in length), with the kinetochores attached to the spindle microtubules (Figure 1, D and E, step II). The timing of entry into mitosis of our epitope-tagged strain was unchanged compared with the parental *cdc25-22* strain (data not shown). Cells were then chilled at 4°C for 30 min. At this point, the spindles collapsed and microtubules were absent (Figure 1, D and E, step III). Live analysis confirmed that microtubules were completely depolymerized (data not shown). The spindles reassembled within minutes after rapid rewarming to 25°C; however, after the cold shock and reassembly process, the kinetochores were often not aligned between the two SPBs in fixed cells (Figure 1, D and E, step IV). Live cell analysis revealed no tubulin signal between the "lost" sister kinetochores and the spindle. In fixed cells, we defined sister kinetochores as "lost" when one or more kinetochore pairs were not located on the spindle between the two SPBs but instead at a distance of at least 0.4 μm from the nearest SPB. A panel of representative images of fixed cells (taken 2 min after recovery from cold shock) is shown in Figure 1E, step IV. The average distance from the lost kinetochores to the nearest SPB was analyzed in fixed cells and was found to be 1 μm $\pm$ 0.51 μm (n = 41; see *Materials and Methods*; Figure 1F). We quantified the percentage of prometaphase/metaphase cells showing an unattached kinetochore in fixed cell samples taken at 60-s intervals after rewarming. The process of kinetochore search, capture, and retrieval was found to be extremely rapid, as 50% of the lost kinetochores were retrieved within 3.5 min (Figure 1G). A similar rapid time frame was observed for this process in a wild-type background as opposed to *cdc25-22* (data not shown). These observations suggest that eukaryotic cells have established an extremely efficient mechanism to recapture lost chromosomes.

Intranuclear Microtubules Are Required to Recapture Lost Kinetochores

To visualize individual kinetochore–microtubule interactions, we followed the process of recovery of lost kinetochores by live microscopy. We observed that INMs (as judged by their localization within the nuclear envelope, Figure 1, A and B) were able to recapture lost kinetochores and pull them to their respective SPB (Figure 2A, Movie 1, retrieval by end-on pulling, defined as when the kinetochore and the end of the INM move toward the SPB simultaneously). Interestingly, upon contact between the INM and the lost kinetochore, the two sisters can be visualized, suggesting that capture occurs via a single kinetochore (Figure 2A, frames 45–60 s, red arrows). We next analyzed the movement of the lost sister kinetochores and the length of the INM with time (Figure 2B) and found that the kinetochores moved toward the SPB at a speed comparable to that of INM depolymerization, 6 μm/min. Analysis of other movies allowed us to calculate the average maximum speed of kinetochore retrieval as being 4.45 $\pm$ 0.4 μm/min (n = 16). Retrieval speeds ranged from 2.9 to 7 μm/min and were compatible with the rate of microtubule shrinkage often observed in astral microtubules or interphase cytoplasmic microtubules. Surprisingly, we found that in a small percent of cases (6–9% depending on experiments) sister kinetochore retrieval to the SPB could be accomplished by an alternative mechanism before anaphase onset and spindle elongation (Figure 3A; Movie 2; retrieval by lateral sliding, defined as when the speed of kinetochore retrieval and the shrinkage rate of the INM were uncoordinated). In this case, we observed sliding of the kinetochore along the INMs, whereas the maximum speed of the kinetochore was found to be within the same range as that seen during end-on pulling.

Micrographic magnifications and kinetic analyses of the capture process are presented in Figure 3, B and C. It should be noted that kinetochore capture and the retrieval to the SPB took less than 1 min in several movies (Figure 3C). We observed some pauses in microtubule depolymerization during the retrieval process (green track in Figure 3C) before the lost kinetochores (red) moved to the SPB. Capture and sliding of the lost kinetochore (Figure 3, A and B; yellow arrows in Figure 3B) was followed by a pause at the SPB (Figure 3, A and C), which lasted ~3 min before migration to the metaphase plate took place (Figure 3, A, D, and E).

Both spindle morphogenesis and sister kinetochore recapture require SPB function. However, the recovery process is not complete until the recaptured kinetochores rejoins the other chromosomes grouped at the spindle midzone. We found that this phase took much longer (on average 10 min) than kinetochore retrieval (on average 2 min). We analyzed this event, using the distal SPB as a Euclidian reference (Figure 3E, reference SPB in black, captured SPB in blue, size of the metaphase plate in black, central spindle indicated by the black dashed line). As soon as the lost kinetochore pair

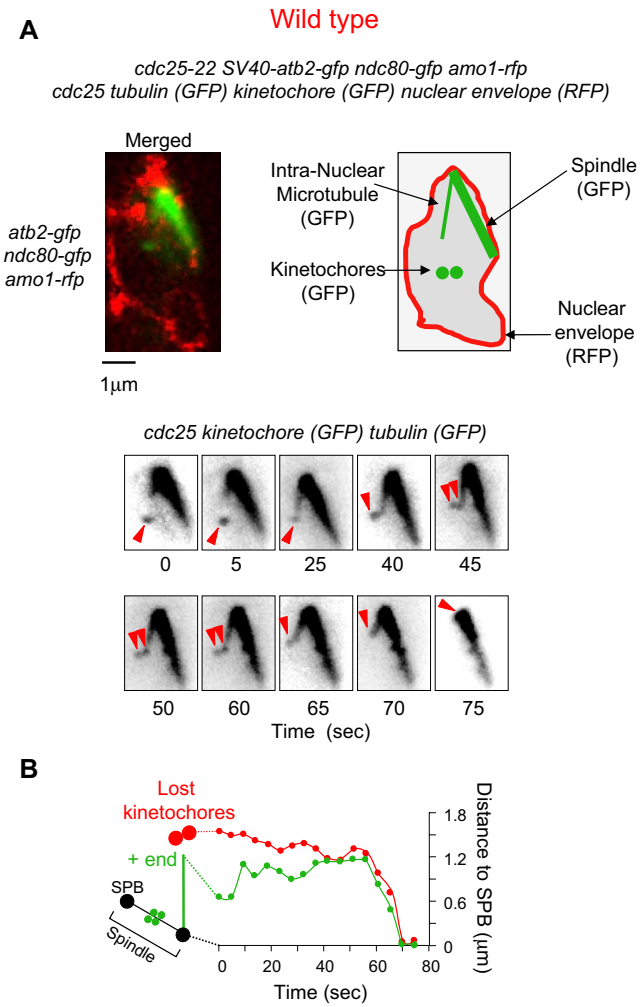

Figure 2. (A) Image series showing sister kinetochore recapture and retrieval in metaphase *cdc25-22 amo1-rfp ndc80-gfp SV40-gfp-atb2 cdc11-cfp* cells during recovery from cold shock. Top, merged image of microtubules, kinetochore and the nuclear envelope showing kinetochore recapture (kinetochores, green dots; nuclear envelope, red). Bottom, still image series taken from Movie 1. (B) Analysis of kinetochore retrieval after cold shock in the *cdc25-22 amo1-rfp ndc80-gfp SV40-gfp-atb2 cdc11-cfp* cell shown above. The position of the lost kinetochore pair is indicated in red and the plus end of the INM is shown in green. The position of the SPB involved in the recapture was used as the reference point.

left the SPB in the direction of the central spindle it splits into two (Figure 3D, yellow arrows, time 9.4 and 11 min). Although the sister kinetochores regained the metaphase plate after 10 min, anaphase A did not take place until 17 min. During this period, spindle elongation was initiated at a reduced speed of 0.25 μm/min compared with the full anaphase B spindle elongation rate of 0.85 μm/min. It should be noted that throughout the entire process of the sister kinetochore recapture and relocalization, the metaphase plate is maintained by the four remaining kinetochores, indicating that the metaphase plate can be initiated and maintained even in the presence of unattached chromosomes.

It is well documented that kinetochore capture takes place early in mitosis, before anaphase onset. Thus, we were extremely surprised to observe an additional mechanism of sister kinetochore capture in anaphase cells (Supplementary Figure 2, retrieval by SPB-independent spindle incorporation), which we also observed in a wild-type background after cold shock. The anaphase spindles observed in these experiments originate from the mitotic cells, which normally enter anaphase after rebuilding their spindle, occasionally showing an unattached kinetochore pair. This phenomenon was quite rare (only 2% of the cases), demonstrating the efficiency of chromosome recapture in metaphase cells. However, we found that in the few cells that escape the mitotic checkpoint with an unattached kinetochore, the lost kinetochore can be recaptured by the spindle microtubules directly, rather than by the INMs (Supplementary Figure 1A; Supplementary Movie 1). We analyzed the dynamics of this unusual way of chromosome capture as described above and found that the incorporation of the lost kinetochores into the spindle was associated with a reduced rate of spindle elongation (0.33 mm/min compared with 0.7–1.20 mm/min during unperturbed mitosis, Supplementary Figure 1B). Again, incorporation of the lost kinetochore was not immediately followed by anaphase onset, which took place 4 min before chromosome segregation. Because the lost kinetochore pair split into two sisters after incorporation into the spindle, we hypothesize that bipolar attachment was achieved at this time, allowing chromosome separation. Interestingly, we never observed direct kinetochore rescue by central spindle microtubules before the onset of anaphase, even when the unattached chromosome was located in close proximity to the spindle (data not shown). Although we cannot exclude the possibility that this mechanism operates during metaphase, we have only ever observed INM-dependent recapture before anaphase. However, as we show here, when anaphase has been executed unattached chromosomes can be directly retrieved by the central spindle microtubules.

From these experiments, we conclude that the INMs are required during early mitosis to prevent chromosome loss and that kinetochore retrieval to the SPB is achieved primarily by microtubule depolymerization (end-on attachment) and to a lesser degree by kinetochore "sliding", defined as when the kinetochore reached the SPB before the end of the INM. In the unlikely event of cells escaping the mitotic checkpoint with an unattached chromosome, a second capture mechanism can take place, which uses the spindle microtubules during anaphase.

The Minus-End–directed Motor dhc1 Is Not Essential for Kinetochore Recapture

Our observations suggest that kinetochore retrieval to the SPB can be performed both by microtubule depolymerization and kinetochore sliding. These two mechanisms may exist to enhance either the efficiency and/or the fidelity of kinetochore retrieval. In particular, we wondered what factors regulate kinetochore sliding along the microtubules. Because ATP-driven motor proteins could be involved in this process, we tested whether the minus-end–directed motor dynein may be involved in the process of kinetochore recapture. As described above, we analyzed the average maximum speed of sister kinetochores retrieval after capture by the INM in a *cdc25-22 dhc1Δ SV40-gfp-atb2 ndc80-gfp amo1*-rfp strain. We found that the speed of kinetochore recapture was not significantly affected in the *dhc1* mutant as opposed to wild-type cells (Figure 4F; average maximum speed 4.11 ± 0.51 μm/min, n = 19). In the absence of the dynein heavy chain Dhc1, kinetochores were successfully retrieved either by end-on pulling (Figure 4, A and B, red arrows; Movie 3) or by lateral sliding (Figure 4, C and D, red arrows; Movie 4). The relative proportion of these two mechanisms was indistinguishable from that seen in the wild type

(~10% of recapture by sliding in a *dhc1* mutant; Figure 4E). However, in a small percentage of cells (10%), laterally attached kinetochores moved erratically toward the SPB, pausing and moving again (Figure 4, C and D), and some even failed to be retrieved (Supplementary Figure 3, A and B). Interestingly, in wild-type cells the rate of shrinkage of the INMs which did not capture a kinetochore (gray bar, Figure 4G, 2.98 ± 0.5 μm/min, n = 15) was reduced compared with the INMs which did capture a kinetochore (red bar, Figure 4G; 4.45 ± 0.4 μm/min, n = 16). This finding was unchanged in *dhc1* delete cells, showing that microtubule depolymerization after kinetochore capture is not promoted by Dhc1 (gray bar, Figure 4G, 2.88 ± 0.56 μm/min, n = 15; red bar; Figure 4G; 4.11 ± 0.51 μm/min, n = 19). Importantly, in 30% of *dhc1* delete cells (data not shown) and as recently described by Grischuk and coworkers, after retrieval to the SPB, the kinetochores stayed in close proximity to the SPB and some failed to migrate to the central spindle suggesting that dynein is required for correct biorientation and segregation (Courtheoux *et al.*, 2007; Grishchuk, 2007). In agreement with these observations, a similar analysis made on fixed cells revealed a greater proportion of unattached chromosomes in the *dhc1* mutant as opposed to wild-type cells (data not shown), suggesting that although dynein is not essential for kinetochore retrieval, it contributes to the efficiency and fidelity of this process.

The Minus-End–directed Motor klp2 Promotes Microtubule Depolymerization during Kinetochore Recapture

It has been very recently established that in budding yeast the transport of captured kinetochores along microtubules is promoted by Kar3, a kinesin-14 family member, whereas this kinesin plays a minor role in the process of recapture by end-on pulling (Tanaka *et al.*, 2005, 2007). In fission yeast, the direct homolog of Kar3 is the minus-end–directed kinesin Klp2. Therefore, we analyzed the process of sister kinetochore retrieval in a *cdc25-22 klp2Δ SV40-gfp-atb2 ndc80-gfp*

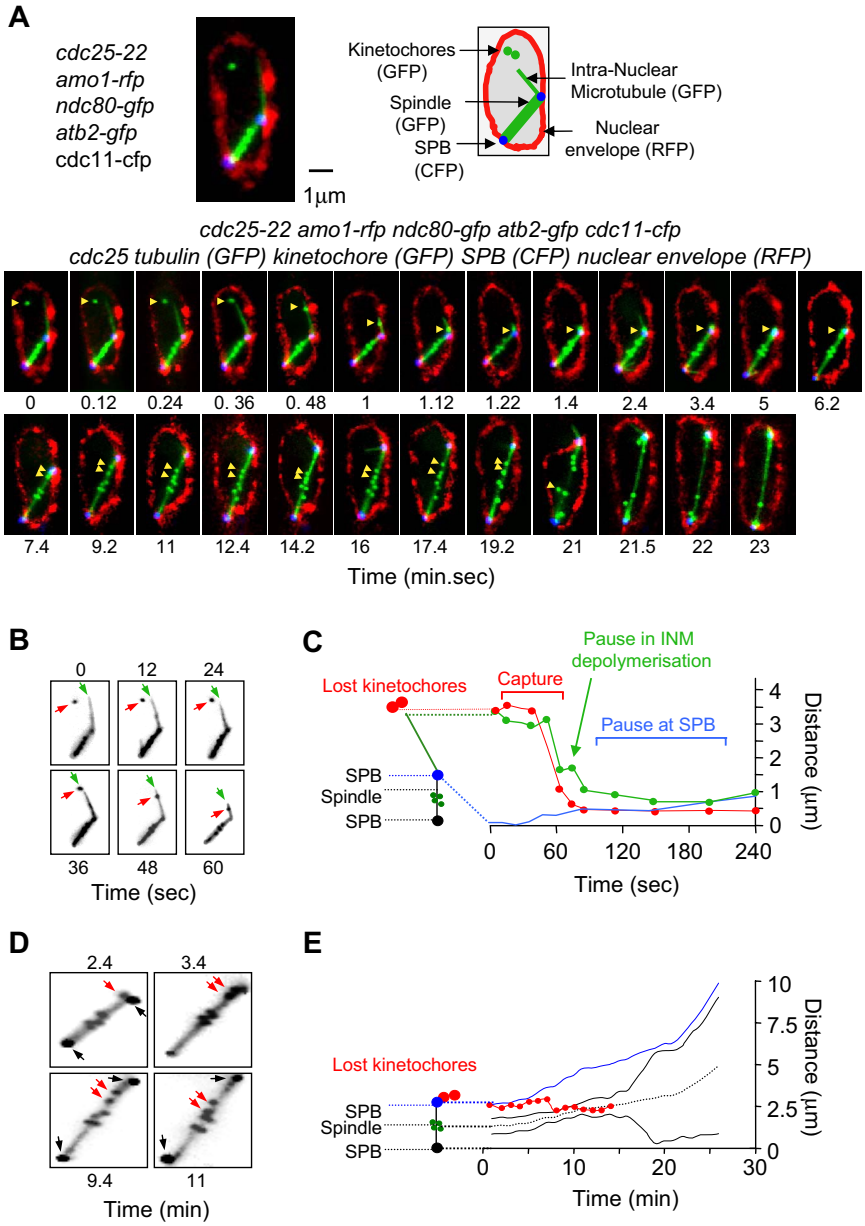

Figure 3. (A) Image series of a metaphase *cdc25-22 amo1-rfp ndc80-gfp SV40-gfp-atb2 cdc11-cfp* cell during recovery from cold shock (Movie 2). (B) Enlarged image of the metaphase *cdc25-22 amo1-rfp ndc80-gfp SV40-gfp-atb2 cdc11-cfp* cell shown in A, where we can visualize the sliding of the lost kinetochore (INM, green arrows; kinetochore, red arrow). (C) Analysis of the sliding of the lost kinetochore (in red) on the INM (in green). The position of the SPB involved in capture of the kinetochore was used as the reference for the analysis. (D) Enlarged image of the *cdc25-22 amo1-rfp ndc80-gfp SV40-gfp-atb2 cdc11-cfp* cell shown in A, where we can visualize the lost kinetochore (red arrows) moving from the SPB to the metaphase plate (SPBs, black arrows). (E) Analysis of the lost kinetochore (in red) moving from the SPB (in blue) to the central spindle (black dashed line). The maximum distance between the four kinetochores (green dots) already positioned on the spindle is indicated by the black traces. The position of the SPB (closed circle) not involved in the capture of the lost kinetochore was used as the reference for the analysis. The position of the SPB that captured the lost kinetochore (in blue) represents the spindle length.

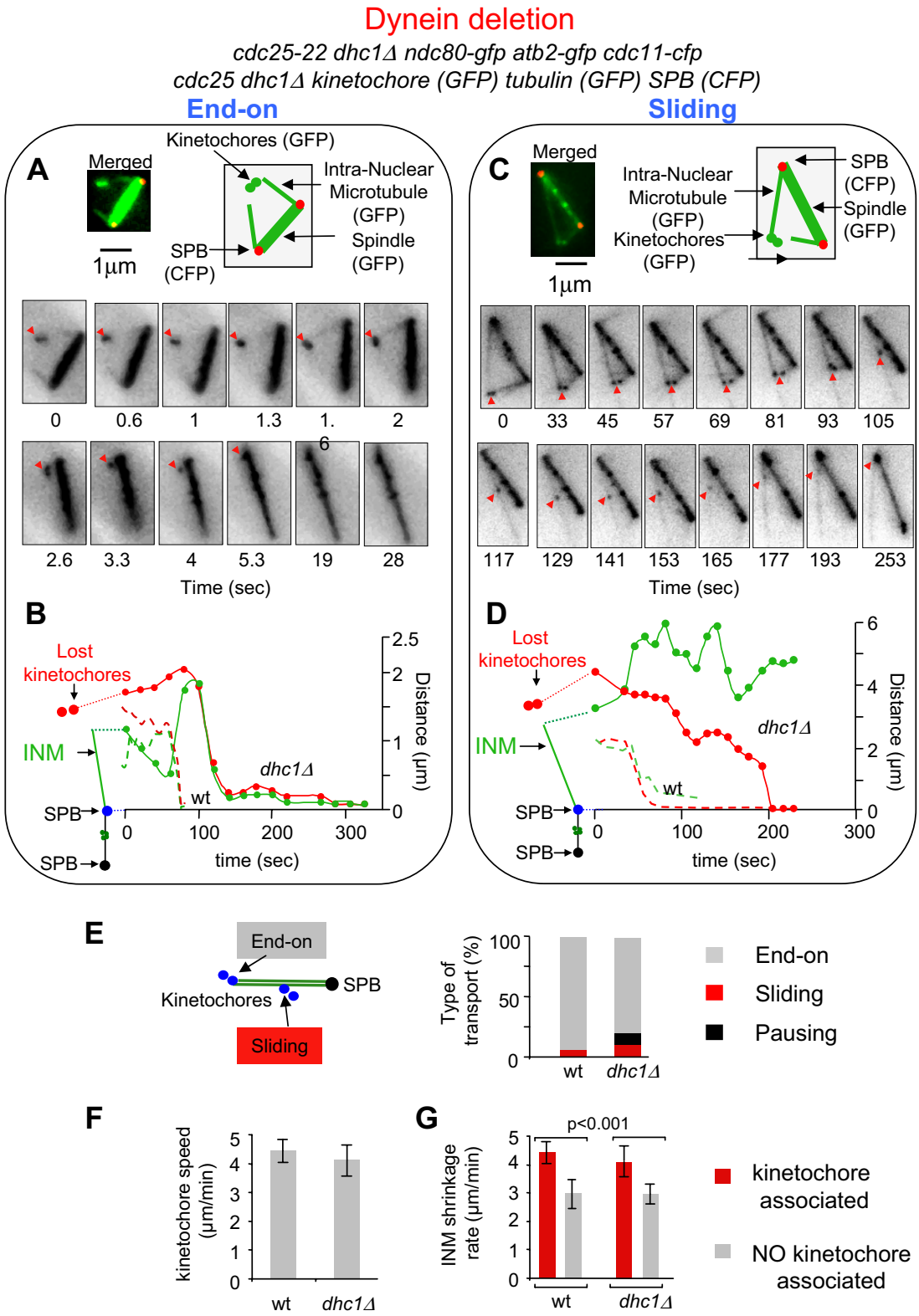

Figure 4. (A) Image series showing end-on kinetochore retrieval in metaphase *cdc25-22 dhc1Δ amo1-rfp ndc80-gfp SV40-gfp-atb2 cdc11-cfp* cells during recovery from cold shock (Movie 3). Top, merged image of microtubules, kinetochores, and SPBs showing kinetochore recapture. Bottom, sequential negative images of the kinetochores and microtubules. (B) Analysis of kinetochore recovery after cold shock in the *cdc25-22 dhc1Δ amo1-rfp ndc80-gfp SV40-gfp-atb2 cdc11-cfp* cell shown above. The position of the lost kinetochore pair is indicated in red and the plus end of the INM is shown in green. The position of the SPB involved in the recapture was used as the reference point. The dashed lines represent the kinetochore/INM plus-end trajectories of the wild-type end-on retrieval shown in Figure 2. (C) Image series showing kinetochore recapture by microtubule sliding in metaphase *cdc25-22 dhc1Δ amo1-rfp ndc80-gfp SV40-gfp-atb2 cdc11-cfp* cells during recovery from cold shock (Movie 4). Top, merged image of microtubules, kinetochores, and SPBs showing kinetochore recapture. Bottom, sequential

amo1-rfp strain. In this mutant, both recapture mechanisms were present (Figure 5, A and B, end-on retrieval and Movie 5; Figure 5, C and D, retrieval by sliding and Movie 6). In Figure 5, A and B, the kinetochore initially interacts laterally with the INM in a sliding position, but this is subsequently transferred to an end-on attachment followed by microtubule catastrophe and end-on pulling of the kinetochore. Strikingly, in the *klp2* mutant lost kinetochores were mainly retrieved by sliding (77%, Figure 5, C and D) rather than by end-on attachment (33%, Figure 5, A and B); the relative proportions of these two mechanisms were reversed compared with those seen in either the wild-type or the dynein mutant. We found that the average maximum speed of kinetochore retrieval was significantly reduced in the *klp2* mutant as opposed to wild-type cells regardless of whether it occurred by sliding or end-on pulling (Figure 5F; average maximum speed 2.16 ± 0.6 μm/min, n = 15 as opposed to 4.45 ± 0.4 μm/min, n = 16 for wild-type cells). In agreement with these observations, we found that the rate of INM shrinkage after sister kinetochore capture during end-on pulling was also significantly reduced in the *klp2* mutant compared with wild-type cells (Figure 5G; 2.43 ± 0.6 μm/min, n = 5 as opposed to 4.45 ± 0.4 μm/min, n = 16). Interestingly, the rate of shrinkage of the INMs which did not capture a pair of kinetochores was similar in both wild-type and *klp2* delete cells (2.74 ± 0.7 μm/min, n = 12 as opposed to 2.98 ± 0.5 μm/min, n = 15), suggesting that Klp2 promotes microtubule depolymerization after kinetochore capture.

Although kinetochore sliding was the main mode used for sister kinetochore retrieval in the *klp2* mutant, the average speed of the sliding kinetochore was significantly reduced compared with that of wild-type cells (1.4 μm/min for *klp2* as opposed to 6 μm/min for wild type; n = 10). Therefore, we conclude that when INM shrinkage is affected, lateral sliding becomes the essential mode of transport for the retrieval of lost kinetochores.

Dynein Cooperates with Klp2 in the Kinetochore Sliding Mechanism

Because lateral sliding was not completely abrogated in the Klp2 mutant, we wondered if dynein could cooperate with Klp2 in the sliding process. Therefore, we analyzed kinetochore retrieval in a *cdc25-22 dhc1*Δ *klp2*Δ *SV40-gfp-atb2 ndc80-gfp cdc11-cfp* strain. Again, in the double mutant, both recapture mechanisms were present (Figure 6, A and B, end-on retrieval; Figure 6, C and D, retrieval by sliding). We found that the average maximum speed of kinetochore retrieval was significantly reduced in the double mutant as opposed to wild-type cells regardless of whether it occurred by sliding or end-on pulling (Figure 6F; average maximum speed 2.5 ± 1 μm/min, n = 11 as opposed to 4.45 ± 0.4 μm/min, n = 16 for wild-type cells). Thus, the sister kinetochore retrieval speed in the double mutant was reduced to a speed similar to that seen in the *klp2* mutant (2.16 ± 0.6 μm/min). Interestingly, in the *klp2* mutant lost kinetochores were mainly retrieved by sliding (77%, Figure 5, C and D), whereas in the *dhc1*Δ *klp2*Δ double mutant lost kinetochores were mainly retrieved by an end-on mechanism (18% sliding, Figure 6E). Because in the *klp2*Δ *dhc1*Δ double mutant the sliding mechanism is no longer predominant and the speed of sliding is reduced, our observations strongly suggest that dynein cooperate with Klp2 in this process.

The Dam1 Complex Is Essential for Kinetochore Retrieval

We next studied what other factors promote the retrieval of kinetochores to the SPB. Although the Dam1 complex is not required for kinetochore sliding in budding yeast (Tanaka *et al.*, 2005), it has recently been shown to play a key role in kinetochore retrieval by end-on pulling (Tanaka *et al.*, 2007). Indeed, the complex forms a ring encircling microtubules in vitro, which might tether the kinetochores to the microtubule ends. We and others have shown that DASH components such as Dam1 and Ask1 decorate the plus-end extremities of INMs in fission yeast (Sanchez-Perez *et al.*, 2005). We therefore investigated the efficiency of kinetochore retrieval after cold shock in a *dam1*Δ *SV40-gfp-atb2 ndc80-gfp amo1*-rfp strain by live cell videomicroscopy. We found that the *dam1* mutant cells had difficulties in reforming a bipolar spindle after cold shock. Instead, a high percentage of broken spindles with lost kinetochores were observed (67%, Figure 7A; Movie 7). Lost kinetochores were successfully captured by these spindle fragments, but they were maintained with end-on attachments and failed to move along the microtubules in the direction of the SPB (Figure 7, A and B; Movie 7). Correctly re-formed bipolar spindles nucleating INMs were also able to capture lost kinetochores by end-on attachment, but also failed to retrieve them to the SPB (Figure 7, C and D). These results were confirmed in more than 20 cells, where captured kinetochores were observed to remain at a standstill (absence of directed movement) for more than 20 min, and only erratically and undirected movement were observed (Figure 7, E and F; maximum undirected kinetochore speed was 0.68 ± 0.2 μm/min, n = 5; average kinetochore speed during a 5-min time lapse was 0.11 μm/min), after which the signal was too weak to permit further analysis (Figure 7, A and C). In agreement with these observations, we found that the rate of INM shrinkage after kinetochore capture was greatly reduced in the *dam1* mutant compared with wild-type cells (Figure 7G; 0.68 ± 0.2 μm/min, n = 5 as opposed to 4.45 ± 0.4 μm/min, n = 16). Interestingly, the rate of shrinkage of the INMs that did not capture a kinetochore was also greatly reduced compared with wild-type cells (1.21 ± 0.5 μm/min, n = 9, as opposed to 2.98 ± 0.5 μm/min, n = 15).

Therefore, as in the *klp2*Δ cells, these experiments suggest that the Dam1 complex may be involved in the destabilization of INMs upon kinetochore attachment, but is not required for kinetochore capture. Unlike Klp2, Dam1 may also be required for the destabilization of INMs that are unattached to a kinetochore (Figure 7G). Unlike the minus-end–directed kinesin Klp2, Dam1 is also essential for kinetochore transport by the "sliding" mechanism during kinetochore retrieval. Together, our observations demonstrate that kinetochore capture in fission yeast is performed via two mech-

Figure 4 (cont). negative images of the kinetochores and microtubules. (D) Analysis of kinetochore recovery after cold shock in the *cdc25-22 dhc1*Δ *amo1-rfp ndc80-gfp SV40-gfp-atb2 cdc11-cfp* cell shown above. The position of the lost kinetochore pair is indicated in red and the plus end of the INM is shown in green. The position of the SPB involved in the recapture was used as the reference point. The dashed lines represent the kinetochore/INM plus-end trajectories of the wild-type sliding retrieval shown in Figure 3. (E) Left panel, schematic representation of the type of transport used to retrieve the kinetochores. Right panel, type of transport of the retrieved kinetochores (%) in wild-type cells as opposed to *dhc1*Δ cells. In red, retrieval by microtubule sliding. In gray, retrieval by end-on microtubule depolymerization. In black, retrieval with kinetochore pausing or at a standstill (F) Average maximum speed of kinetochore retrieval in wild-type or *dhc1*Δ cells. (G) Average INM shrinkage rate in wild-type or *dhc1*Δ cells in the presence (red) or absence (gray) of an associated kinetochore. Error bars, 99% confidence intervals.

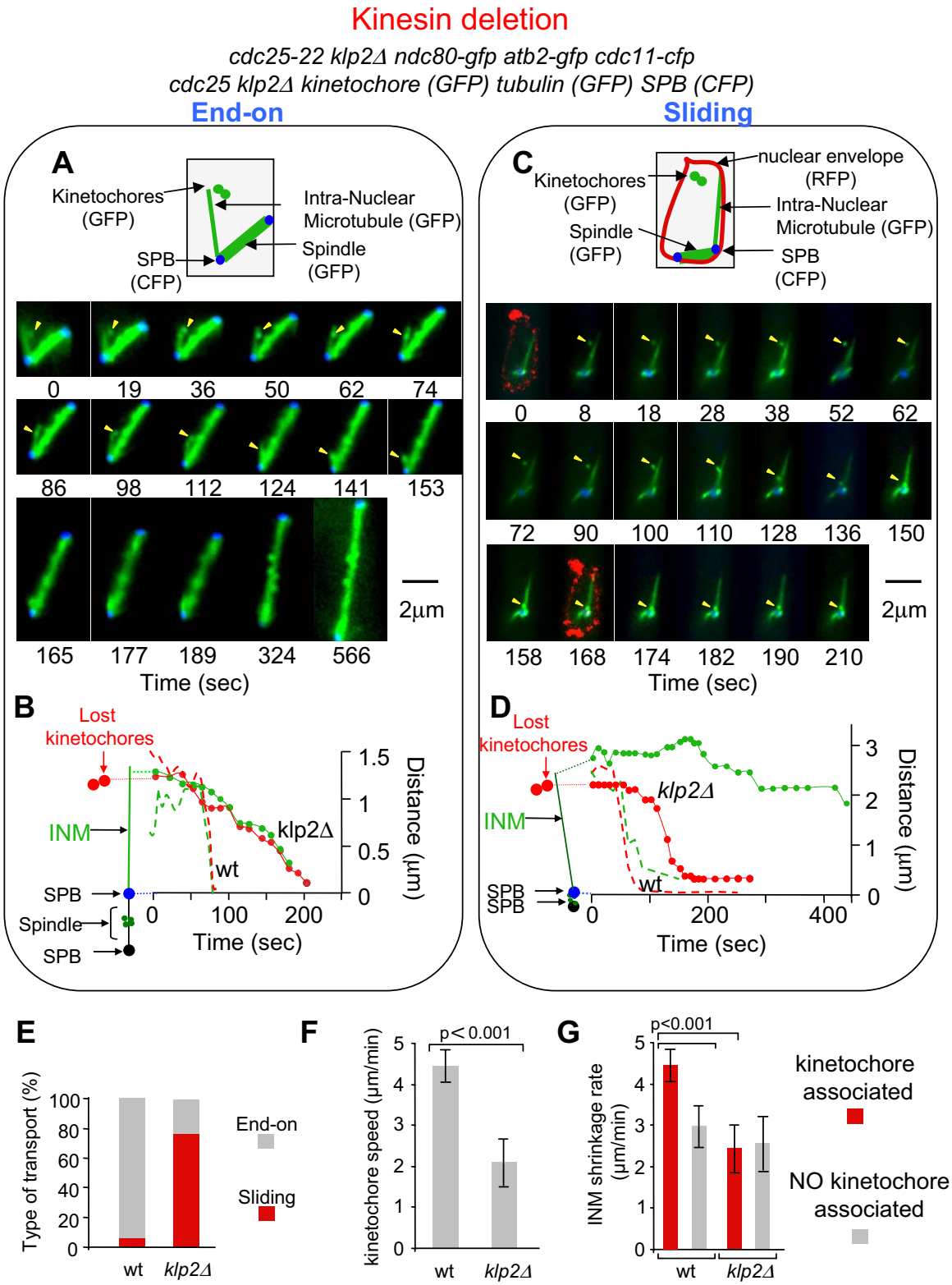

Figure 5. (A) Image series showing end-on kinetochore retrieval in metaphase *cdc25-22 klp2Δ amo1-rfp ndc80-gfp SV40-gfp-atb2 cdc11-cfp* cells during recovery from cold shock (Movie 5). Top, merged image of microtubules, kinetochore and SPBs showing kinetochore recapture. Bottom, sequential images of the kinetochores, microtubules and SPBs. (B) Analysis of kinetochore recovery after cold shock in the *cdc25-22 klp2Δ amo1-rfp ndc80-gfp SV40-gfp-atb2 cdc11-cfp* cell shown above. The position of the lost kinetochore pair is indicated in red and the plus end of the INM is shown in green. The position of the SPB involved in the recapture was used as the reference point. The dashed lines represent the kinetochore/INM plus-end trajectories of the wild-type end-on retrieval shown in Figure 2. (C) Image series showing kinetochore recapture by microtubule sliding in metaphase *cdc25-22 klp2Δ amo1-rfp ndc80-gfp SV40-gfp-atb2 cdc11-cfp* cells during recovery from cold shock (Movie 6). Top, merged image of microtubules, kinetochore and SPBs showing kinetochore recapture. Bottom, sequential

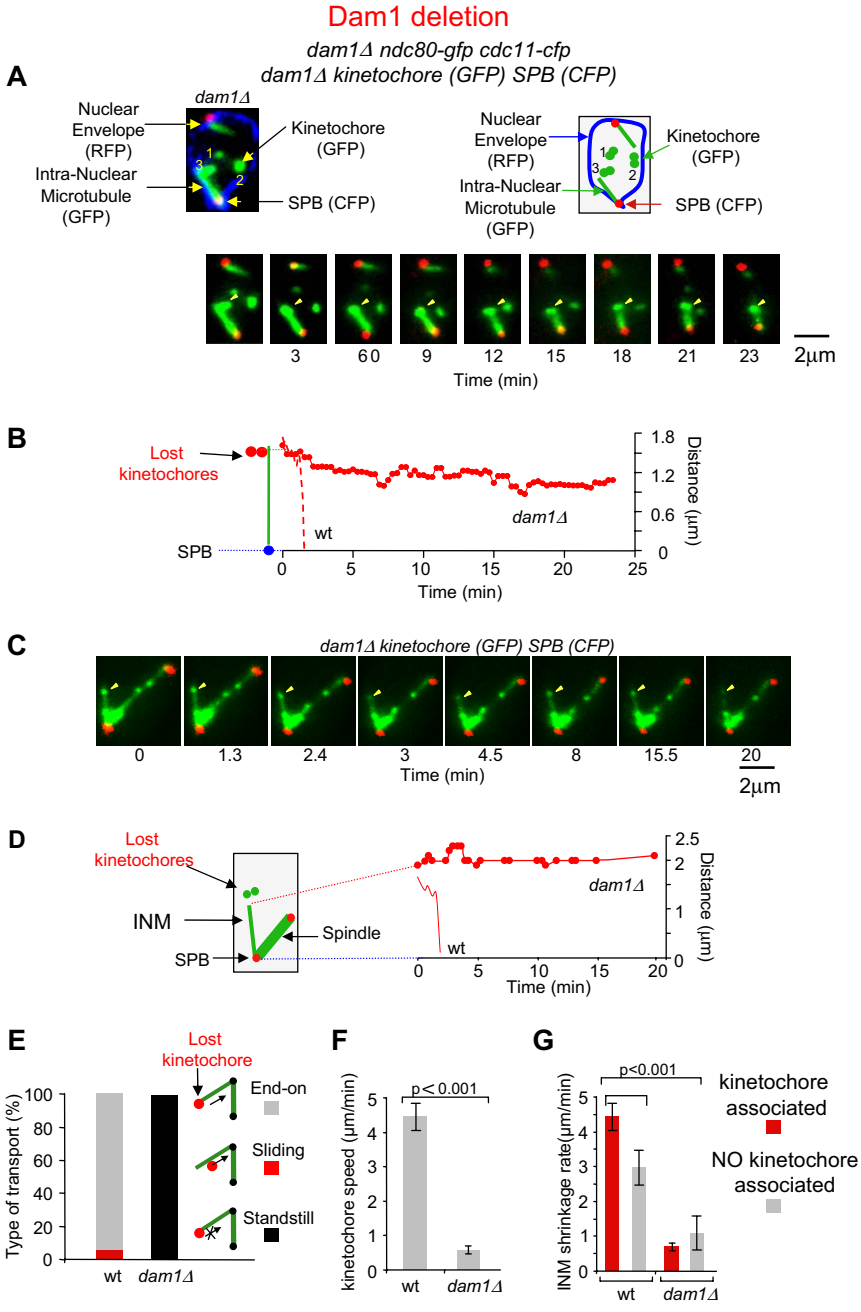

Figure 7. (A) Image series showing an attempt at end-on kinetochore retrieval in metaphase *dam1Δ amo1-rfp ndc80-gfp SV40-gfp-atb2 cdc11-cfp* cells during recovery from cold shock (Movie 7). Top, merged image and cartoon of microtubules, kinetochores, SPBs and nuclear envelope showing kinetochore recapture. Bottom, sequential images of the kinetochores, microtubules and SPBs. The three pairs of chromosomes are indicated by the numbers 1, 2, and 3. (B) Analysis of kinetochore recovery after cold shock in the *dam1Δ amo1-rfp ndc80-gfp SV40-gfp-atb2 cdc11-cfp* cell shown above. The position of the lost kinetochore pair is indicated in red. The position of the SPB involved in the recapture was used as the reference point. The dashed line represents the kinetochore trajectory of the wild-type end-on retrieval shown in Figure 2. (C) Image series showing an attempt at kinetochore recapture by an INM in metaphase *dam1Δ amo1-rfp ndc80-gfp SV40-gfp-atb2 cdc11-cfp* cells during recovery from cold shock. Merged image of microtubules, kinetochores, and SPBs (D) Analysis of kinetochore recovery after cold shock in the *dam1Δ amo1-rfp ndc80-gfp SV40-gfp-atb2 cdc11-cfp* cell shown above. The position of the lost kinetochore is indicated in red. The position of the SPB involved in the recapture was used as the reference point. The dashed line represents the kinetochore trajectory of the wild-type retrieval shown in Figure 2. (E) Type of transport of the retrieved kinetochore (%) in wild-type cells as opposed to *dam1Δ* cells. In red, retrieval by microtubule sliding. In gray, retrieval by end-on microtubule depolymerization. In black, stationary kinetochores (F) Average maximum speed of kinetochore retrieval in wild-type or *dam1Δ* cells. (G) Average INM shrinkage rate in wild-type or *dam1Δ* cells in the presence (red) or absence (gray) of an associated kinetochore. Error bars, 99% confidence intervals.

Figure 5 (cont). images of the kinetochores, microtubules and SPBs. (D) Analysis of kinetochore recovery after cold shock in the *cdc25-22 klp2Δ amo1-rfp ndc80-gfp SV40-gfp-atb2 cdc11-cfp* cell shown above. The position of the lost kinetochore pair is indicated in red and the plus end of the INM is shown in green. The position of the SPB involved in the recapture was used as the reference point. The dashed lines represent the kinetochore/INM plus end trajectories of the wild-type sliding retrieval shown in Figure 3. (E) Type of transport of the retrieved kinetochore (%) in wild-type cells as opposed to *klp2Δ* cells. In red, retrieval by microtubule sliding. In gray, retrieval by end-on microtubule depolymerization. (F) Average maximum speed of kinetochore retrieval in wild-type or *klp2Δ* cells. (G) Average INM shrinkage rate in wild-type or *klp2Δ* cells in the presence (red) or absence (gray) of an associated kinetochore. Error bars, 99% confidence intervals.

anisms, end-on pulling and microtubule sliding, which are both dependent on Dam1.

Dam1 and Klp2 Colocalize with the Kinetochore during Its Transport to the SPB

Because Dam1 and Klp2 are both involved in sister kinetochore retrieval in fission yeast, we decided to investigate their localization during the process of kinetochore recapture after cold shock. We first created a *cdc25-22 dam1-gfp ndc80-cfp* strain to allow us to follow the localization of Dam1 and the lost kinetochore during its retrieval to the SPB by live cell videomicroscopy. We found that during kinetochore retrieval Dam1 colocalized with the kinetochores on the spindle and at the extremity of the INMs, as previously reported (Sanchez-Perez *et al.*, 2005). We also found that the

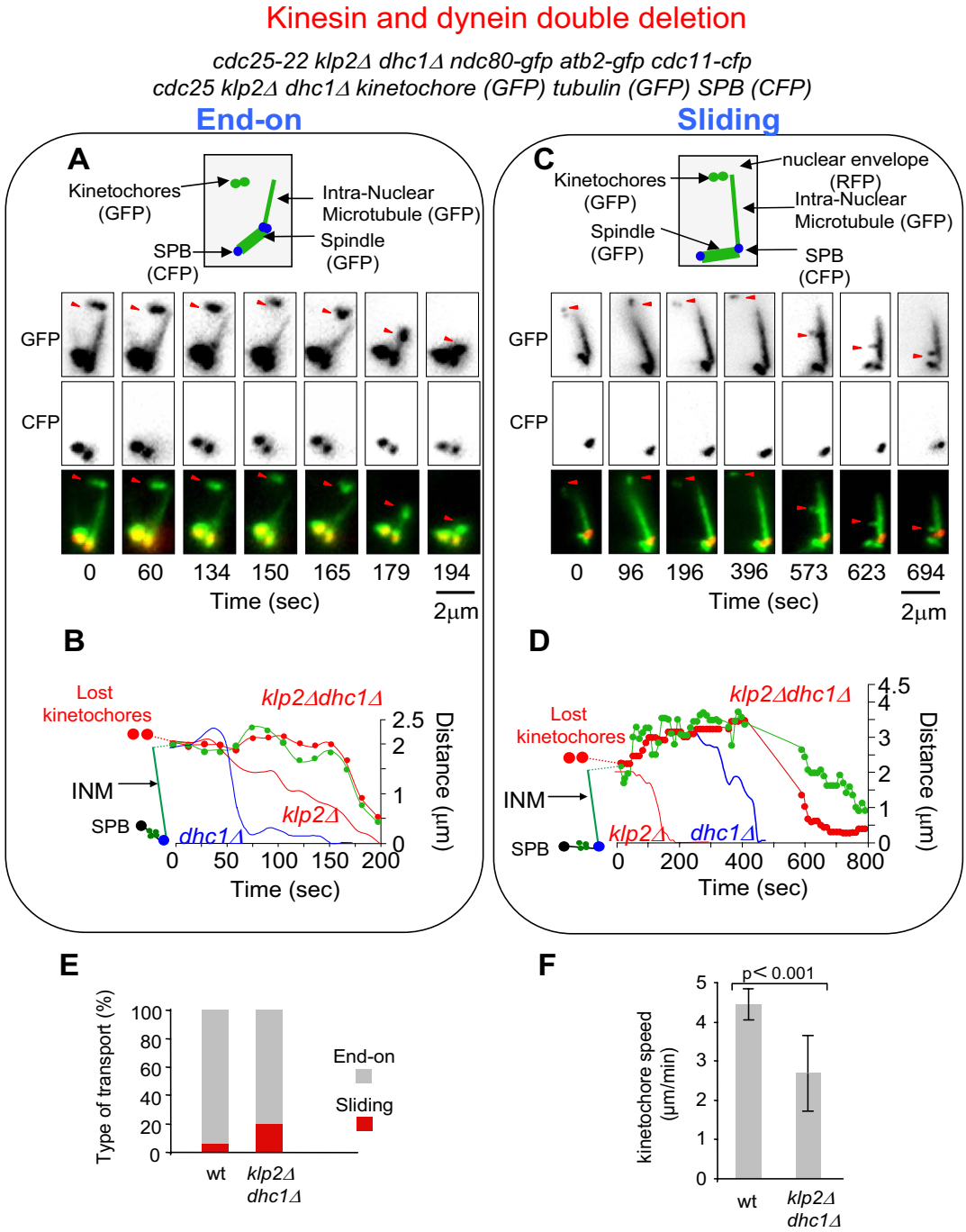

Figure 6. (A) Image series showing end-on kinetochore retrieval in metaphase *cdc25-22 dhc1*Δ *klp2*Δ *ndc80-gfp SV40-gfp-atb2 cdc11-cfp* cells during recovery from cold shock. Images of microtubules and kinetochores (GFP) and SPBs (CFP) or merged images showing kinetochore recapture. (B) Analysis of kinetochore recovery after cold shock in the *cdc25-22 dhc1*Δ *klp2*Δ *ndc80-gfp SV40-gfp-atb2 cdc11-cfp* cell shown above. The position of the lost kinetochore pair is indicated in red and the plus end of the INM is shown in green. The position of the SPB involved in the recapture was used as the reference point (blue SPB). The solid red line represents the kinetochore trajectories of the *klp2*Δ end-on retrieval shown in Figure 4 and the solid blue line represents the kinetochore trajectories of the *dhc1*Δ end-on retrieval shown in Figure 5. (C) Image series showing kinetochore recapture by microtubule sliding in metaphase *cdc25-22 dhc1*Δ *klp2*Δ *ndc80-gfp SV40-gfp-atb2 cdc11-cfp* cells during recovery from cold shock. Images of microtubules and kinetochores (GFP) and SPBs (CFP) or merged images showing kinetochore recapture. (D) Analysis of kinetochore recovery after cold shock in the *cdc25-22 klp2*Δ *amo1-rfp ndc80-gfp SV40-gfp-atb2 cdc11-cfp* cell shown above. The position of the lost kinetochore pair is indicated in red and the plus end of the INM is shown in green. The position of the SPB involved in the recapture was used as the reference point. The solid red line represents the kinetochore trajectories of the *klp2*Δ sliding retrieval shown in Figure 4 and the solid blue line represents the kinetochore trajectories of the *dhc1*Δ sliding retrieval shown in Figure 5. (E) Type of transport of the retrieved kinetochore (%) in wild-type cells as opposed to *dhc1*Δ*klp2*Δ cells. In red, retrieval by microtubule sliding. In gray, retrieval by end-on microtubule depolymerization. (F) Average maximum speed of kinetochore retrieval in wild-type or *dhc1*Δ *klp2*Δ cells. Error bars, 99% confidence intervals.

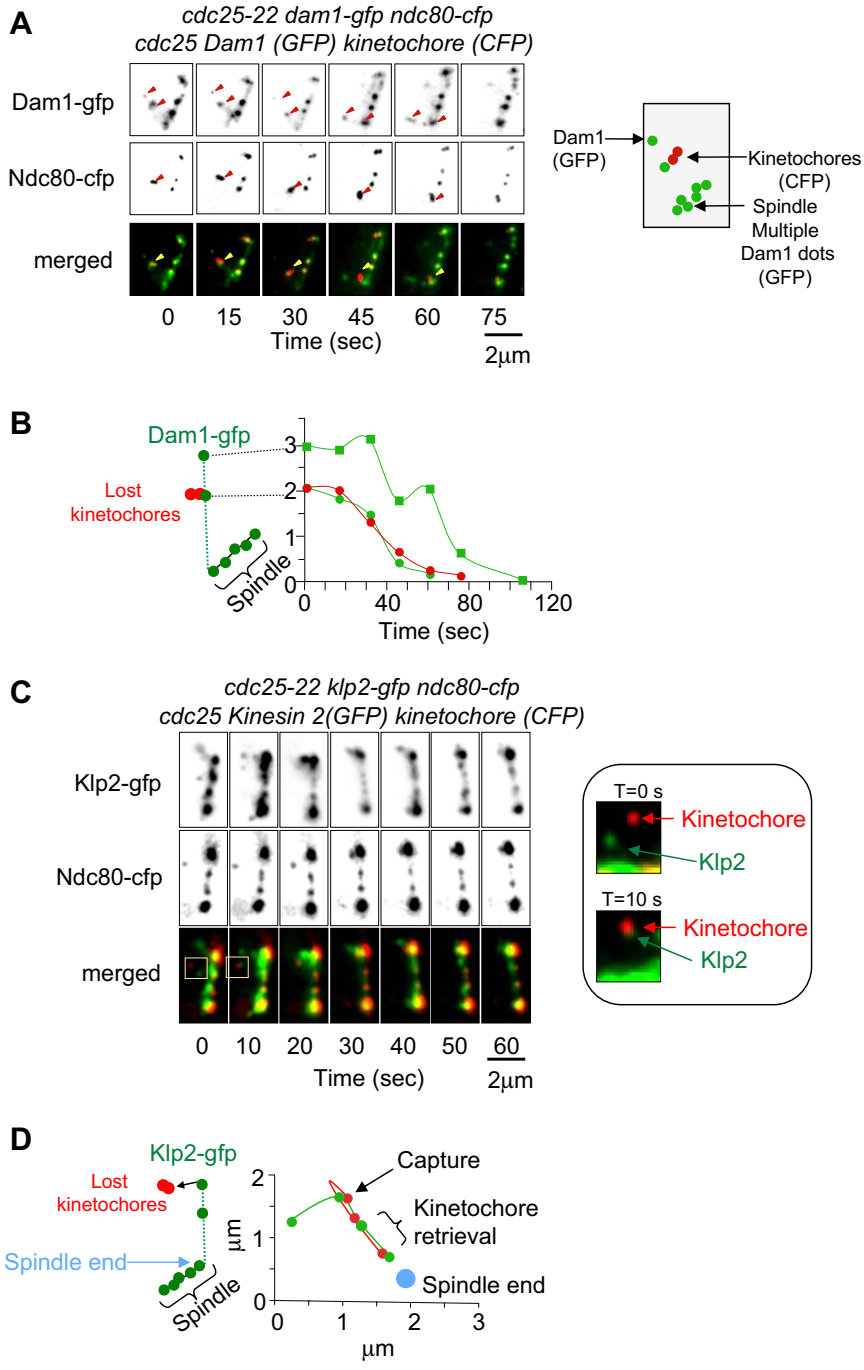

Figure 8. (A) Image series showing kinetochore retrieval by sliding in metaphase *cdc25-22 dam1-gfp ndc80-cfp* cells during recovery from cold shock (Movie 8). Images of Dam1 (GFP) and kinetochores (CFP) or merged images showing kinetochore recapture. (B) Analysis of kinetochore recovery after cold shock in the *cdc25-22 dam1-gfp ndc80-cfp* cell shown above. The position of the lost kinetochore pair is indicated in red and the plus end of the INM, as defined by Dam1-gfp, is shown in green. The position of the SPB (as judged by the extremity of the spindle) involved in the recapture was used as the reference point. (C) Image series showing end-on kinetochore retrieval in metaphase *cdc25-22 klp2-gfp ndc80-cfp cdc11-cfp* cells during recovery from cold shock (Movie 9). Images of Klp2 (GFP) and kinetochores/SPBs (CFP) or merged images showing kinetochore recapture. (D) Tracking analysis of kinetochore recovery after cold shock in the *cdc25-22 klp2-gfp ndc80-cfp cdc11-cfp* cell shown above. The position of the lost kinetochore pair is indicated in red and the plus end of the INM as defined by Klp2-gfp signal is shown in green. The position of the SPB (spindle end) involved in the recapture is indicated as a blue dot.

INMs were either decorated by single dots of Dam1, as shown in Figure 1, or by several dots of Dam1 (Figure 8, A and B, red arrows, Movie 8). In Figure 8, A and B, we present an example of kinetochore retrieval by sliding where Dam1 continuously colocalizes with (or is in close proximity to) the lost kinetochore during its transport to the SPB. This was also true when kinetochores were retrieved by end-on pulling (data not shown) or when klp2 was deleted (Supplementary Movie 1). Therefore in fission yeast, as opposed to budding yeast, Dam1 always colocalizes with the captured kinetochore during its transport along the microtubule. This result is in agreement with our previous observation that Dam1 is required both for sliding and end-on retrieval of lost kinetochores.

We next examined the localization of Klp2 using by live cell videomicroscopy of a *cdc25-22 klp2-gfp ndc80-cfp cdc11-cfp* strain. As observed for Dam1, we found that after kinetochore recapture Klp2 colocalized with the kinetochores on the spindle and at the extremity of the INMs. Again, Klp2 either decorated the INMs as single or as multiple dots. Before kinetochore recapture, Klp2 was not detectable on the lost kinetochores in our experiments (t = 0, see magnification), but colocalized with the kinetochore as soon as it was captured by the INM, and during its transport (t = 10, see magnification, Figure 8, C and D; Movie 9). This result is in agreement with our previous observations showing that Klp2 participates in kinetochore retrieval in fission yeast.

Intranuclear Microtubules Extend Preferentially in the Direction of the Kinetochores

Our observations show that the search, capture and retrieval of lost kinetochores occur within a 5-min interval. The accuracy and rapidity of this process led us to ask if kinetochore capture is inherently random or if INMs extend preferentially from the SPB closest to the unattached kinetochore. To answer this question, we analyzed INM behavior before kinetochore retrieval in 25 individual movies. We first determined whether a single INM or multiple INMs were produced before kinetochore recapture by performing multiple Z-stacks (15 Z stacks, 0.22 μm apart) and 3D reconstructions in live *cdc25-22 SV40-gfp-atb2 ndc80-gfp amo1-rfp* cells (Figure 9A; Movie 10). Within the limits of detection of our system, as shown in Movie 8, the large majority of cells exhibited a single microtubule emanating from the SPB. We therefore decided to analyze the length and the direction of this microtubule compared with the position of the lost kinetochore. We first determined whether the production of INMs during this phase was isotropic or anisotropic compared with the position of the lost kinetochore. Surprisingly, we found that 100% of INMs were produced on the same side of the spindle and that this side was adjacent to the lost sister kinetochores (Figure 9B, left). This was not due to the presence of the nuclear envelope, which could potentially interfere with INM production, because cells subjected to identical spindle damage but without lost kinetochores showed a normal isotropic distribution of INMs (Figure 9B, right). The nucleation of INMs positioned closer to the nuclear envelope was not affected, although these INMs were shorter. A large majority (68%) of all INMs were produced by the SPB proximal to the kinetochore, whereas the 32% that were produced by the distal SPB were oriented in the direction of the lost sister kinetochores (Figure 9B, left). We next determined the distance between the SPB and the lost sister kinetochores and compared this to the size of the adjacent INM immediately before kinetochore recapture for 23 movies. The data reported in Figure 9C shows that INM size correlates well with the SPB–kinetochore distance. We also determined the angle (α) between the SPB producing the INM and the lost kinetochore and the angle between the INM and the spindle (β) immediately before recapture (Figure 9, D and E). Once again, we found a significant correlation between these two angles (r = 0.73, Figure 9E). The average angle between the INM and the sister kinetochores was centered to 0 $\pm$ 10° (Figure 9F). These results suggest that the length and orientation of the INM, even in the case of unsuccessful capture, is determined by the position of the lost chromosomes.

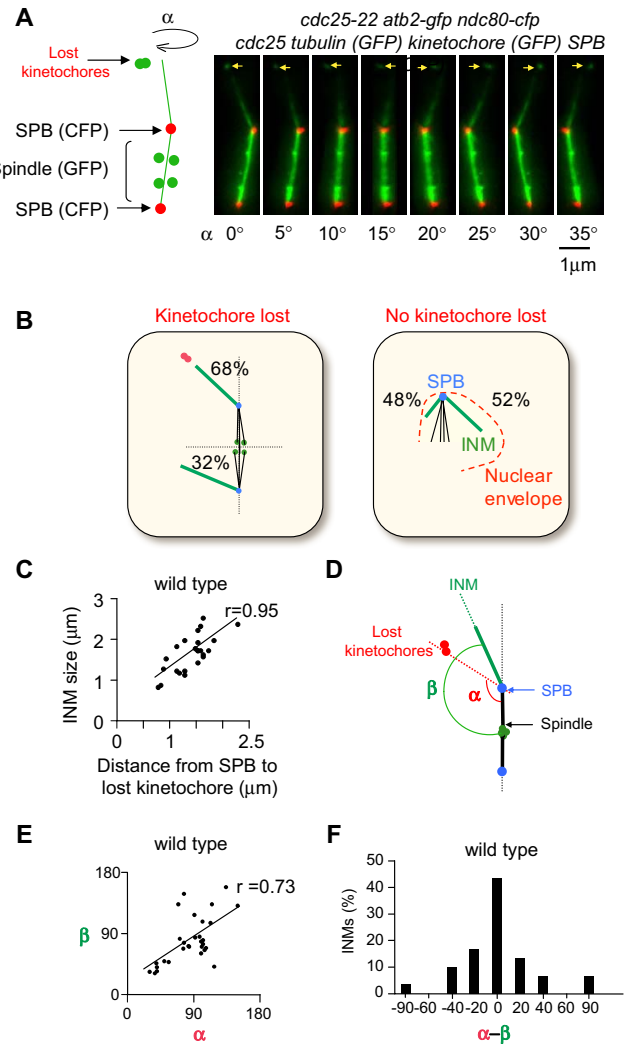

Figure 9. (A) Three-dimensional reconstruction of 15 stacks of 0.22-μm steps in a single cell showing kinetochore recapture, viewed from different angles. The SPBs appear in red, the microtubules and kinetochores in green (Movie 10). (B) The left panel shows a statistical analysis of the INM nucleation zones with the nuclear space divided into quarters. The lost kinetochore (in red) was arbitrarily positioned in the top left quadrant and the positions of the INMs were quantified. The SPBs are indicated in blue, the spindle in black and the INM and spindle-associated kinetochores in green. The right panel shows a statistical analysis of the INMs nucleation zones when the nuclear space is divided in two. One side of the spindle is close to the nuclear envelope (in red), and the positions of the INMs were quantified. The SPBs are indicated in blue, the spindle in black and the INM and spindle-associated kinetochores in green. (C) Analysis of SPB-kinetochore distance and INM length before capture of the lost kinetochore (D) Schematic representation of the mitotic apparatus. The spindle is shown in black, the INMs in green, and the lost kinetochore in red. The SPBs are represented as open circles and the nuclear envelope is shown in green. (E) Analysis of the distribution of the differences between the angle from spindle to the lost kinetochore (α) and the angle formed by the INMs and spindle (β) before capture. (F) Distribution analysis of the angular gaps between the kinetochore and INM directions, centered at the SPB as shown in C (α-β).

DISCUSSION

The maintenance of genetic integrity requires faithful sister chromatid segregation at the onset of mitosis. In fission yeast, the presence of pre-anaphase INMs have been reported but their precise role remains obscure (Zimmerman *et al.*, 2004). We hypothesized that INMs provide a read-out of spindle damage during mitosis and may therefore be required to prevent chromosome loss. The recapture of lost kinetochores by microtubules has been visualized in very few cell types, including budding yeast, newt lung cells, and Ptk2 cells, largely due to technical reasons. In this study we have used live videomicroscopy to show that the INMs are "kinetochore hunter" microtubules that are required to recapture lost chromosomes. In agreement with these observations, components of the DASH complex such as Dam1 or Ask1, which are required for correct microtubule-kinetochore attachment, are exclusively located on the INMs, whereas other microtubule-binding proteins such as Mal3 decorate both astral microtubules and INMs.

In this report, we found that the poleward movement of the lost sister kinetochores to the SPB can occur in two ways: by lateral "sliding" of the kinetochore (defined as when the kinetochore reaches the SPB before the plus end of the INM) or by end-on pulling of the kinetochore by the INM (defined as when the kinetochore and the plus end of the INM move to the SPB simultaneously). We have previously established that in fission yeast the centromeres congress to the spindle midzone before sister chromatid separation (Tournier *et al.*, 2004). We now show that after retrieval of the lost chromosome to the SPB, the two sister kinetochores move toward the central spindle and align on the metaphase plate with the two other chomosomes. As soon as the two sisters left the SPB, they were resolved into two individual dots on the spindle, suggesting that biorientation may occur before alignment on the metaphase plate. However, we found that neither the retrieval of lost sister kinetochores to the SPB nor their congression to the metaphase plate were sufficient to induce anaphase onset (which only occurred 7 min later). Therefore, it is likely that these two events are not the only requirements for the initiation of anaphase onset. Indeed, it is possible that biorientation is only established when the chromosomes align on the metaphase plate and that the apparent separation of the two sisters after leaving the SPB results from pulling forces produced by a plus-end–directed motor. Recent findings support this hypothesis (Kapoor *et al.*, 2006).

Our experiments show that lost kinetochores can be retrieved by an alternative central spindle microtubule-dependent mechanism in anaphase cells. Although it is possible that this mechanism may also operate in metaphase cells, we never observed this type of recapture before the onset of anaphase in any of our experiments, suggesting that kinetochore retrieval in metaphase cells is uniquely performed by mechanisms that involve transit via the SPB. However, after anaphase (as judged by the presence of two of the chromosomes segregated to the SPBs, one lost chromosome with unseparated sisters), microtubules can retrieve the lost kinetochores to the central spindle. In this case, the process of kinetochore retrieval and biorientation does not necessitate passage via the SPB. It is likely that cohesion is specifically maintained on the lost chromosome to avoid kinetochore separation within the nucleoplasm, which would inevitably result in segregation defects, even after recapture. Indeed, we found that in this situation the spindle checkpoint protein Mad2 was specifically maintained on the lost chromosome but absent from the others already at the poles (unpublished observations). An alternative possibility is that both the establishment of tension and the degradation of cohesion may be required to segregate the kinetochores and that therefore segregation can only occur when chromosomes are correctly bioriented on the spindle. We found that this type of recapture was a rare event (only 2% of the cases in wild-type cells), which makes it difficult to study but demonstrates that the spindle assembly checkpoint and kinetochore retrieval during metaphase are highly efficient in living cells. Although it was originally thought that lost chromosomes could only be recaptured during early mitosis, it is clear that an alternative mechanism can operate in early anaphase. Whether this mechanism requires the function of the spindle assembly checkpoint is at present unknown. These observations illustrate the complexity but flexibility of the mechanisms that prevent genomic instability.

In budding yeast a Kar3-dependent lateral sliding mechanism is the primary mode of retrieval of lost kinetochores (Tanaka *et al.*, 2005). Our observations show that in fission yeast, as in other organisms, lost kinetochores also use the

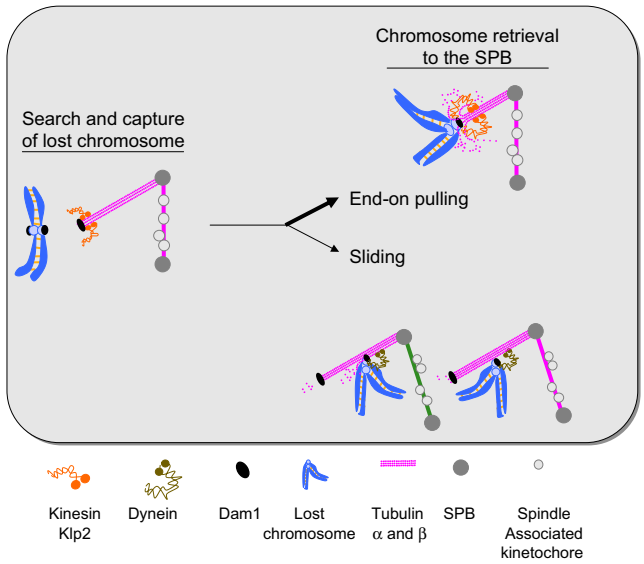

Figure 10. Schematic representation of the different modes of kinetochore retrieval during mitotic progression.

INMs as a track to increase the efficiency of their retrieval. However, in fission yeast kinetochore retrieval is mainly achieved by end-on attachment and INM depolymerization rather than by kinetochore sliding. Our results are in agreement with those of Grishchuk and McIntosh (2006), who recently reported that the maximum rate of poleward kinetochore movement was unaffected by the deletion of any or all of the minus-end–directed motors: Klp2 (Kar3 homolog), Pkl1, and the dynein Dhc1, which led them to suggest that end-on pulling is the only mechanism operating in fission yeast. Significantly, although we found that end-on pulling was the major mechanism used for the retrieval of lost kinetochores, retrieval by lateral sliding can and does occur in wild-type cells (Figure 10). Whether INMs are in fact bundles of microtubules and that kinetochore-associated microtubules selectively shrink within the bundle, giving the impression that a sliding mechanism operates in fission yeast, is at present unclear (Figure 10). Nevertheless, two mechanisms for retrieval are observed, raising the question of the necessity for these two mechanisms. The first hypothesis that we propose as an answer to this question is that one or the other may increase the speed of return to the SPB of the lost kinetochore, once captured. However, we found no significant differences in the maximum speed of kinetochore retrieval either by end-on pulling or by sliding. A second possible advantage of using a sliding mechanism is that multiple lost chromosomes located close to each other could use the same microtubule "track" to be retrieved at the same time, therefore increasing the effectiveness of the system. Alternatively, it is possible that this sliding mechanism represents a back-up to prevent chromosome loss in the unlikely event of reduced microtubule catastrophe.

In budding yeast, Kar3 is essential to drive poleward lateral sliding. Similarly, the only minus-end–directed motor, which contributes to the effectiveness of kinetochore movements in fission yeast is the kinesin Klp2 (Grishchuk and McIntosh, 2006), whereas dynein seems to participate in later events such as chromosome biorientation and segregation (Courtheoux *et al.*, 2007; Grishchuk, 2007). In their studies Grishchuk and McIntosh were unable to visualize kinetochore/microtubule attachment during retrieval to the SPB.

We therefore readdressed the role of Klp2 in this process, simultaneously observing the spindle, INMS, kinetochores, and SPBs, and found that the main mode of kinetochore transport used by cells deleted for Klp2 was lateral sliding, rather than end-on attachment as in wild-type cells or the dynein mutant. In wild-type cells, the INM shrinkage rate is significantly reduced upon kinetochore capture. In the *klp2* mutant, the INM shrinkage rate is relatively unaffected by kinetochore attachment, indicating a role for *klp2* in controlling INM dynamics. Thus, the dominance of sliding as a retrieval mechanism in the *klp2* delete cells reflects the relative stability of the INMs, whereas the reduction in kinetochore return speed seen in this mutant may be due to the lack of Klp2 motor activity. Interestingly, in the double mutant *klp2*Δ *dhc1*Δ the sliding mechanism is no longer predominant, and the speed of sliding is reduced, which may suggest that dynein cooperates with Klp2 in the sliding process. If INMs are in fact bundles of microtubules and that kinetochore-associated microtubules selectively shrink within the bundle, it is unclear how dynein and Klp2 could cooperate in this process.

In vitro experiments have suggested that several Dam1 complexes could gather together and form a ring structure, which could then encircle and move along microtubules. More recently, in vivo experiments performed in budding yeast support a model in which the Dam1 complex tethers the kinetochores to the microtubules and plays a crucial role in converting microtubule depolymerization to kinetochore pulling force as initially proposed in vitro. In budding yeast, the end-on retrieval of kinetochores requires the Dam1 complex, whereas kinetochore retrieval by sliding along microtubules still operates normally in these cells. During the course of this study Franco *et al.* (2007) have shown that the Dam1 complex is required for the retrieval of unclustered kinetochores in fission yeast. In their study, they demonstrate that cells deleted for the γ-tubulin complex component (γ-TuC) Mto1 show defects in kinetochore clustering and report that in this genetic background kinetochores can be retrieved by an end-on mechanism or by lateral attachment followed by end-on retrieval. Interestingly, they never observed retrieval by a sliding mechanism, despite the fact that the INMs in the *mto1* mutant are extremely stable, as judged by the reduced speed of kinetochore retrieval in their model. It is likely that the discrepancies between their study and ours are due to the altered INM dynamics present in the *mto1* mutant.

Strikingly, in agreement with the Franco *et al.* (2007) study, we found that in fission yeast kinetochore retrieval was completely abrogated in a *dam1* delete strain, although lost kinetochores were correctly captured. We interpret this result as a consequence of the role of Dam1 in either directly or indirectly promoting INM shrinkage because we found that the INM shrinkage rate was greatly reduced in this mutant. Although laterally attached kinetochores were observed, they failed to move along the side of the INM and instead remained at a standstill for long periods of time. Surprisingly, we found that the *dam1* mutant still displays end-on attachment, as opposed to the Franco *et al.* (2007) study. It is possible that the plus ends of the INMs in the *mto1* mutant are not normal. Indeed, Zimmerman and Chang (2005) reported that Tip1 (a CLIP-170 protein) accumulates abnormally at the MT plus ends in interphase *mto1* mutant cells. They also found an abnormal localization of the Kelch repeat protein Tea1 on the spindle, suggesting that the defects in the *mto1* mutant are not restricted to the interphase microtubules (Zimmerman and Chang, 2005). The requirement for Dam1 for kinetochore retrieval is intriguing, because as opposed to budding yeast, Dam1 is not an essential gene in fission yeast, although *dam1*Δ cells lose chromosomes at high rate. It is possible that the kinesins Klp5/Klp6, which are not required for kinetochore recapture (Franco *et al.*, 2007), cooperate with Dam1 at anaphase onset to pull chromosomes to the SPBs. Indeed, Sanchez-Perez *et al.* (2005) have shown that the double mutant *klp5*Δ *dam1*Δ is not viable in fission yeast.

Our results point to an essential role for microtubule dynamics in the control of kinetochore retrieval in fission yeast. Indeed, both the Klp2 and Dam1 proteins seem to play an important role in kinetochore-induced microtubule depolymerization and consequently in kinetochore retrieval. Therefore, at least in fission yeast, the control of INM dynamics is central to the mechanisms underlying sister kinetochores search, capture, and retrieval.

In summary, although budding yeast principally uses a Dam1-independent minus-end kinesin-driven movement to retrieve lost kinetochores, fission yeast uses primarily a Dam1-dependent microtubule depolymerization–based mechanism. It is possible that in fission yeast kinetochore retrieval is entirely based on microtubule depolymerization. Indeed, although we find that klp2 and dynein cooperate in the sliding mechanism, we cannot exclude the possibility that INMs are in fact bundles of microtubules and that kinetochore-associated microtubules selectively shrink within the bundle, giving the impression that a sliding mechanism operates in fission yeast. If this model is correct, deletion of Klp2 would reduce the speed of kinetochore sliding by reducing the microtubule shrinkage rate, whereas deletion of Dam1 would block all kinetochore movement by blocking attachment–dependent microtubule shrinkage. Our observations have shown that in exponentially growing cells, as has also been described in budding yeast, plus-end–binding proteins such as Mal3 (or Ask1, Dam1) decorate the extremity of the INMs as a single dot, suggesting that no overlapping microtubules are present. However, during the process of cold shock and kinetochore retrieval, we found that Dam1 and Klp2 can decorate the INMs either as single or multiple dots and always colocalize with the kinetochore during its retrieval. Because these dots could either be the plus ends of microtubules within a bundle or other structures along the microtubule (Davis and Wordeman, 2007), we cannot at this time discriminate between these different hypotheses (i.e., kinetochore retrieval by surfing along the INM and kinetochore retrieval by selective microtubule shrinkage within the INM).

Kinetochore capture by microtubules is thought to be random, but if this is the case it is difficult to see how mitosis can be so accurate and how the search and capture of lost chromosomes can be achieved so efficiently (within 2 min for the search and capture phase as opposed to 10 min for metaphase plate formation and anaphase onset). In yeast, which undergoes a closed mitosis, the presence of the nuclear envelope may help to restrict the distance between lost chromosomes and the SPBs. However, in higher eukaryotes, more complicated mechanisms exist. A series of studies have suggested the existence of a "distance" effect of chromatin on microtubules (Dogterom *et al.*, 1996; Carazo-Salas and Karsenti, 2003). Initial experiments from Dogterom *et al.* (1996) have used *Xenopus* egg extracts in an attempt to visualize such an effect. Furthermore, biochemical approaches have suggested that chromatin can generate a Ran-GTP gradient, which affects microtubule nucleation, dynamics, and organization at a distance from chromatin (Bastiaens *et al.*, 2006; Kalab *et al.*, 2006). Finally, Carazo-Salas and Karsenti (2003) have demonstrated that in *Xenopus* egg ex-

tracts, chromatin affects microtubule formation at a distance, inducing the preferential orientation of centrosomal microtubules in its direction. However, in vivo demonstrations of these phenomena have not yet been provided.

In budding yeast, it appears that microtubules do not extend preferentially in the direction of the kinetochores (Tanaka *et al.*, 2005). It is unclear why anisotropy has not been observed in budding yeast, although we can exclude the small size of the nucleus because the size of the metaphase nucleus is similar in these two yeasts. However, our experiments show that unattached chromosomes do indeed affect INM formation (or stability), inducing a preferential distribution of spindle pole body microtubules in their direction. The mechanisms controlling this anisotropy in microtubule formation are at present unknown but may involve the existence of signaling gradients around chromatin as well as the activity of the small GTPase Ran and its effectors (Bastiaens *et al.*, 2006; Kalab *et al.*, 2006).

In conclusion, our work shows that in fission yeast cells intranuclear microtubules are required to recapture lost kinetochores by end-on pulling or microtubule sliding, with both mechanisms contributing to control genetic integrity (Figure 10). It was initially thought that INMs randomly explore the nucleoplasm and capture kinetochores after spindle damage. Our results show without doubt that in fission yeast at least, kinetochore capture is a well-orchestrated process that is organized by the chromosome. Further study of the effect of chromosomes on microtubule nucleation and plus end microtubule dynamics will undoubtedly reveal new mechanisms involved in spindle morphogenesis.

ACKNOWLEDGMENTS

We thank Sir P. Nurse (The Rockefeller University, New York/Cancer Research UK, London), T. Toda (Cancer Research UK, London), P. Tran (Institut Curie, Paris), J. R. McIntosh (University of Colorado, Boulder, CO), X. He (Baylor College of Medicine, TX), and J. Millar (National Institute for Medical Research, London) for supplying strains. We thank J. Hyams, A. Merdes, B. Ducommun, and the members of the LBCMCP for helpful discussions. Y.G. is supported by a postdoctoral fellowship from the Fondation pour la Recherche Médicale. T.C. is supported by a fellowship from La ligue contre le cancer. This work was supported in part by l'Association de la Recherche sur le Cancer (ARC).

REFERENCES

Bastiaens, P., Caudron, M., Niethammer, P., and Karsenti, E. (2006). Gradients in the self-organization of the mitotic spindle. Trends Cell Biol. *16*, 125–134.

Beinhauer, J. D., Hagan, I. M., Hegemann, J. H., and Fleig, U. (1997). Mal3, the fission yeast homologue of the human APC-interacting protein EB-1 is required for microtubule integrity and the maintenance of cell form. J. Cell Biol. *139*, 717–728.

Browning, H., Hackney, D. D., and Nurse, P. (2003). Targeted movement of cell end factors in fission yeast. Nat. Cell Biol. *5*, 812–818.

Busch, K. E., and Brunner, D. (2004). The microtubule plus end-tracking proteins mal3p and tip1p cooperate for cell-end targeting of interphase microtubules. Curr. Biol. *14*, 548–559.

Carazo-Salas, R. E., and Karsenti, E. (2003). Long-range communication between chromatin and microtubules in *Xenopus* egg extracts. Curr. Biol. *13*, 1728–1733.

Cheeseman, I. M., Brew, C., Wolnyiak, M., Desai, A., Anderson, S., Muster, N., Yates, J. R., Huffaker, T. C., Drubin, D. G., and Barnes, G. (2001). Implication of a novel multiprotein complex in outer kinetochore function. J. Cell. Biol. *155*, 1137–1145.

Cheeseman, I. M., Drubin, D. G., and Barnes, G. (2002). Simple centrosome, complex kinetochore: linking spindle microtubules and centromeric DNA in budding yeast. J. Cell. Biol. *157*, 199–203.

Courtheoux, T., Gay, G., Reyes, C., Goldstone, S., Gachet, Y., and Tournier, S. (2007). Dynein participates in chromosome segregation in fission yeast. Biol. Cell *99*, 627–637.

Davis, T. N., and Wordeman, L. (2007). Rings, bracelets, sleeves, and chevrons: new structures of kinetochore proteins. Trends Cell Biol. *17*, 377–382.

Dogterom, M., Felix, M. A., Guet, C. C., and Leibler, S. (1996). Influence of M-phase chromatin on the anisotropy of microtubule asters. J. Cell Biol. *133*, 125–140.

Franco, A., Meadows, J. C., and Millar, J. B. (2007). The Dam1/DASH complex is required for the retrieval of unclustered kinetochores. J. Cell. Sci *120*, 3345–3351.

Gachet, Y., Tournier, S., Millar, J. B., and Hyams, J. S. (2004). Mechanism controlling perpendicular alignment of the spindle to the axis of cell division in fission yeast. EMBO J. *23*, 1289–1300.

Grishchuk, E. L., and McIntosh, J. R. (2006). Microtubule depolymerization can drive poleward chromosome motion in fission yeast. EMBO J. *25*, 4888–4896.

Grishchuk, E. L., Spiridonov, I. S., and McIntosh, J. R. (2007). Mitotic chromosome biorientation in fission yeast is enhanced by dynein and a minus-end-directed, kinesin-like protein. Mol. Biol. Cell *Epub ahead of print*.

Janke, C., Ortiz, J., Tanaka, T. U., Lechner, J., and Schiebel, E. (2002). Four new subunits of the Dam1-Duo1 complex reveal novel functions in sister kinetochore biorientation. EMBO J. *21*, 181–193.

Kalab, P., Pralle, A., Isacoff, E. Y., Heald, R., and Weis, K. (2006). Analysis of a RanGTP-regulated gradient in mitotic somatic cells. Nature *440*, 697–701.

Kapoor, T. M., Lampson, M. A., Hergert, P., Cameron, L., Cimini, D., Salmon, E. D., McEwen, B. F., and Khodjakov, A. (2006). Chromosomes can congress to the metaphase plate before biorientation. Science *311*, 388–391.

Li, Y., Bachant, J., Alcasabas, A. A., Wang, Y., Qin, J., and Elledge, S. J. (2002). The mitotic spindle is required for loading of the DASH complex onto the kinetochore. Genes Dev. *16*, 183–197.

Li, J. M., Li, Y., and Elledge, S. J. (2005). Genetic analysis of the kinetochore DASH complex reveals an antagonistic relationship with the ras/protein kinase A pathway and a novel subunit required for Ask1 association. Mol. Cell. Biol. *25*, 767–778.

Liu, X., McLeod, I., Anderson, S., Yates, J. R., 3rd, and He, X. (2005). Molecular analysis of kinetochore architecture in fission yeast. EMBO J. *24*, 2919–2930.

Maiato, H., DeLuca, J., Salmon, E. D., and Earnshaw, W. C. (2004). The dynamic kinetochore-microtubule interface. J. Cell Sci. *117*, 5461–5477.

McIntosh, J. R., Grishchuk, E. L., and West, R. R. (2002). Chromosome-microtubule interactions during mitosis. Annu. Rev. Cell Dev. Biol. *18*, 193–219.

Merdes, A., and De Mey, J. (1990). The mechanism of kinetochore-spindle attachment and polewards movement analyzed in PtK2 cells at the prophase-prometaphase transition. Eur. J. Cell Biol. *53*, 313–325.

Miranda, J. J., De Wulf, P., Sorger, P. K., and Harrison, S. C. (2005). The yeast DASH complex forms closed rings on microtubules. Nat. Struct. Mol. Biol. *12*, 138–143.

Moreno, S., Klar, A., and Nurse, P. (1991). Molecular genetic analysis of fission yeast *Schizosaccharomyces pombe*. Methods Enzymol. *194*, 795–823.

Rieder, C. L., and Alexander, S. P. (1990). Kinetochores are transported poleward along a single astral microtubule during chromosome attachment to the spindle in newt lung cells. J. Cell Biol. *110*, 81–95.

Sanchez-Perez, I., Renwick, S. J., Crawley, K., Karig, I., Buck, V., Meadows, J. C., Franco-Sanchez, A., Fleig, U., Toda, T., and Millar, J. B. (2005). The DASH complex and Klp5/Klp6 kinesin coordinate bipolar chromosome attachment in fission yeast. EMBO J. *24*, 2931–2943.

Savoian, M. S., Goldberg, M. L., and Rieder, C. L. (2000). The rate of poleward chromosome motion is attenuated in *Drosophila* zw10 and rod mutants. Nat. Cell Biol. *2*, 948–952.

Sharp, D. J., Rogers, G. C., and Scholey, J. M. (2000). Cytoplasmic dynein is required for poleward chromosome movement during mitosis in *Drosophila* embryos. Nat. Cell Biol. *2*, 922–930.

Tanaka, K., Kitamura, E., Kitamura, Y., and Tanaka, T. U. (2007). Molecular mechanisms of microtubule-dependent kinetochore transport toward spindle poles. J. Cell Biol. *178*, 269–281.

Tanaka, K., Mukae, N., Dewar, H., van Breugel, M., James, E. K., Prescott, A. R., Antony, C., and Tanaka, T. U. (2005). Molecular mechanisms of kinetochore capture by spindle microtubules. Nature *434*, 987–994.

Tolic-Norrelykke, I. M., Sacconi, L., Thon, G., and Pavone, F. S. (2004). Positioning and elongation of the fission yeast spindle by microtubule-based pushing. Curr. Biol. *14*, 1181–1186.

Tournier, S., Gachet, Y., Buck, V., Hyams, J. S., and Millar, J. B. (2004). Disruption of astral microtubule contact with the cell cortex activates a Bub1,

Bub3, and Mad3-dependent checkpoint in fission yeast. Mol. Biol. Cell *15*, 3345–3356.

Wang, H. W., Ramey, V. H., Westermann, S., Leschziner, A. E., Welburn, J. P., Nakajima, Y., Drubin, D. G., Barnes, G., and Nogales, E. (2007). Architecture of the Dam1 kinetochore ring complex and implications for microtubule-driven assembly and force-coupling mechanisms. Nat. Struct. Mol. Biol.*14*, 721–726.

Westermann, S., Wang, H. W., Avila-Sakar, A., Drubin, D. G., Nogales, E., and Barnes, G. (2006). The Dam1 kinetochore ring complex moves processively on depolymerizing microtubule ends. Nature *440*, 565–569.

Wu, X., Xiang, X., and Hammer, J. A., 3rd. (2006). Motor proteins at the microtubule plus-end. Trends Cell Biol. *16*, 135–143.

Zimmerman, S., and Chang, F. (2005). Effects of γ-tubulin complex proteins on microtubule nucleation and catastrophe in fission yeast. Mol. Biol. Cell *16*, 2719–2733.

Zimmerman, S., Daga, R. R., and Chang, F. (2004). Intra-nuclear microtubules and a mitotic spindle orientation checkpoint. Nat. Cell Biol. *6*, 1245–1246.